List of Figures

Contents

Chapter 5

Frictional Dynamics

So far we have dealt with frictionless flows, where the dominant balance is between the Coriolis and pressure gradient forces. That was shown to be a rather good approximation for flows away from boundaries (topography, surface of the ocean, side boundaries, etc.) but this balance does not hold anymore when a boundary is approached, and frictional forces become important. The region where frictional terms have to be taken into account is called a *boundary layer* (see Fig.5.1). Here we will consider the following:

- The boundary layer is Boussinesq.

- The boundary layer has a finite depth, δ, that is less than the total depth of the fluid, H. The depth is given by the level at which frictional stresses vanish. Within the boundary layer, frictional terms are important, whereas geostrophic balance holds beyond it.

- Nonlinear time-dependent terms in the equations of motion are negligible, hydrostasy holds in the vertical, and buoyancy is constant, not varying in the horizontal.

In atmosphere and ocean dynamics, where the focus is on rapidly rotating turbulent fluids, this boundary layer is called *Ekman layer*.

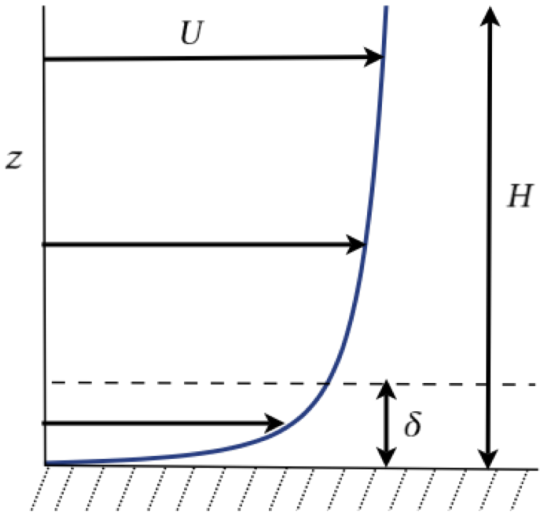

Figure 5.1: *An idealized boundary layer. The boundary layer has thickness δ, within a typical vertical scale H and typical velocity U, which varies rapidly within the boundary layer in order to satisfy the rigid lid boundary condition. [from Vallis (2006)]*

The Ekman Layer
The development of the theories for the wind-driven circulation actually has as a foundation the discovery of the so-called Ekman layer and its circulation. In 1898, the polar explorer Nansen observed that icebergs in the Arctic drifted in a direction to the right of the direction of the surface winds, roughly bewteen 20° and 40° to right of the wind stress. This qualitative observation can be explained by the presence of frictional forces. In fact, wind force applied to the surface of the ocean will try to transmit momentum in the same direction. However, as soon as the fluid starts to move, the Coriolis force will come into action deflecting its movement to the right. Importantly, there is also a frictional force within the fluid that will exert some resistance to this movement, and its direction is opposite to the direction of the fluid. The final balance between wind force, Coriolis and frictional forces, will determine the actual direction and velocity of the fluid, which will be to the right of the wind direction in the northern hemisphere.
As we shall see later, Ekman explained quantitatively how the rotation of the earth was responsible for the deflection of the current which Nansen observed.

5.1 Equations of motion

Let us now include frictional effects in our equations of motion

$$\frac{\mathrm{D}u}{\mathrm{D}t} - fv = -\frac{1}{\rho_0}\frac{\partial p}{\partial x} + F_x \tag{5.1}$$

$$\frac{\mathrm{D}v}{\mathrm{D}t} + fu = -\frac{1}{\rho_0}\frac{\partial p}{\partial y} + F_y \tag{5.2}$$

$$\tag{5.3}$$

Here, F_x and F_y are the friction components per unit mass. Assuming no accelerations in the fluid we are left with a balance between three forces

$$-fv = -\frac{1}{\rho_0}\frac{\partial p}{\partial x} + F_x \tag{5.4}$$

$$fu = -\frac{1}{\rho_0}\frac{\partial p}{\partial y} + F_y. \tag{5.5}$$

We can now make progress on the frictional terms. For a geophysical fluid, the vertical component dominates. The Newton's law of friction states that the friction stress $\boldsymbol{\tau}$, which is the force per unit area, is given by

$$\boldsymbol{\tau} = \mu\frac{\partial \mathbf{u}}{\partial z} = \rho_0\nu\frac{\partial \mathbf{u}}{\partial z} = \rho_0 A_z\frac{\partial \mathbf{u}}{\partial z}, \tag{5.6}$$

where μ is the dynamic viscosity and $\nu = \mu/\rho_0$ the kinematic viscosity. For a turbulent fluid such as the ocean, eddy viscosity A_z (coming about from the Reynolds stresses $-\overline{u'w'} = A_z\partial u/\partial z$) has a value $\sim 10^{-1}$ m^2 s^{-1}.

The eddy friction stress can be expressed in terms of a mass of fluid, where for the vertical component leads to frictional force per unit mass

$$\frac{1}{\rho_0}\frac{\partial \tau}{\partial z} = \frac{1}{\rho_0}\frac{\partial}{\partial z}\left(\rho_0 A_z\frac{\partial u}{\partial z}\right) = A_z\frac{\partial^2 u}{\partial z^2}. \tag{5.7}$$

Our equations of motion thus reduce to

$$-fv = -\frac{1}{\rho_0}\frac{\partial p}{\partial x} + A_z\frac{\partial^2 u}{\partial z^2} \tag{5.8}$$

$$fu = -\frac{1}{\rho_0}\frac{\partial p}{\partial y} + A_z\frac{\partial^2 v}{\partial z^2}. \tag{5.9}$$

Or simply

$$\boxed{\mathbf{f}\times\mathbf{u} = -\frac{1}{\rho_0}\nabla_z p + A\frac{\partial^2 \mathbf{u}}{\partial z^2}}. \tag{5.10}$$

The momentum equation in the vertical is the hydrostatic balance, and the set is completed with mass continuity, $\nabla\cdot\mathbf{u} = 0$.

The Ekman number

We now apply the usual scaling arguments to the equations and obtain the Ekman number

$$\mathrm{Ek} = \left(\frac{A}{f_0 H^2}\right), \tag{5.11}$$

which determines the importance of frictional terms in the horizontal equations. For interior flows, $Ek < 1$, and the flow is geostrophic. Within the Ekman layer, $Ek \geq 1$, and friction is important. The difference between the geostrophic equations and the equations of motion when frictional effects are retained is thus clear.

This implies that the vertical velocities w are not negligible within the boundary layer, near the sea surface and bottom. Friction terms are small enough to be neglected only in the interior of the ocean. If we do not neglect the friction term in the momentum equation this means that the friction term is comparable in size to the Coriolis term

$$A_z \frac{\partial^2 u}{\partial z^2} \simeq f u \tag{5.12}$$

A scaling analysis reveals that

$$A_z (U/H^2) \simeq f U \tag{5.13}$$

For typical values $A_z = 10^{-1}$ m^2 s^{-1} and $f = 10^{-4} s^{-1}$ we get

$$H^2 \simeq \frac{A_z U}{f U} = 10^{-1}/10^{-4} = 10^3 \mathrm{m}^2. \tag{5.14}$$

A typical boundary layer is in the order of $H \simeq 30$ m and frictional effects can be felt up to a 100 m or so.

Momentum balance

We write the velocity field and the pressure field as the sum of interior geostrophic part and a boundary layer correction:

$$\mathbf{u} = \mathbf{u_g} + \mathbf{u_E}, \qquad p = p_g + p_E, \tag{5.15}$$

where the Ekman layer corrections are negligible away from the boundary layer. In the fluid interior we have, by hydrostatic balance, $\frac{\partial p_g}{\partial z} = 0$, because we have considered the fluid to have constant buoyancy $b = -g\rho'/\rho_0$. In the boundary layer, we still have $\frac{\partial p_g}{\partial z} = 0$ and, to satisfy

hydrostasy, $\frac{\partial p_E}{\partial z} = 0$. But because p_E vanishes away from the boundary, $p_E = 0$ everywhere. This implies that there is no boundary layer in the pressure field. For the Ekman layer then, the horizontal momentum equation becomes

$$\mathbf{f} \times \mathbf{u_E} = A_z \frac{\partial^2 \mathbf{u}}{\partial z^2}, \tag{5.16}$$

the dominant force balance in the Ekman layer is thus between the Coriolis force and friction.

We can now estimate the depth over which the Ekman layer extends. Recalling the Ekman number:

$$\mathrm{Ek} = \frac{A_z}{\Omega d^2} \simeq 1, \tag{5.17}$$

this implies that $d = (A_z/\Omega)^{1/2}$. With typical values $A = 10^{-1}$ m^2 s^{-1} and $\Omega = 10^{-4}$ s^{-1}, we get a boundary layer of the order of 30 m.

5.2 Integral properties of the Ekman layer

Let's now deduce the properties of the Ekman layer without specifying the frictional stress tensor τ_{ij}.

The Ekman mass transport

The frictional-geostrophic balance is

$$\mathbf{f} \times \mathbf{u} = -\frac{1}{\rho_0} \nabla_z p + \frac{1}{\rho_0} \frac{\partial \boldsymbol{\tau}}{\partial z}, \tag{5.18}$$

where $\boldsymbol{\tau}$ is zero at the edge of the Ekman layer. In the Ekman layer we have

$$\mathbf{f} \times \mathbf{u_E} = \frac{1}{\rho_0} \frac{\partial \boldsymbol{\tau}}{\partial z}. \tag{5.19}$$

As we seek properties for the entire boundary layer, let's integrate over its thickness

$$\mathbf{f} \times \int_{Ek} \rho_0 \mathbf{u_E} \, \mathrm{d}z = \boldsymbol{\tau}_T - \boldsymbol{\tau}_B, \tag{5.20}$$

where subscripts T and B are for the stresses at the top and bottom of the Ekman boundary layer.

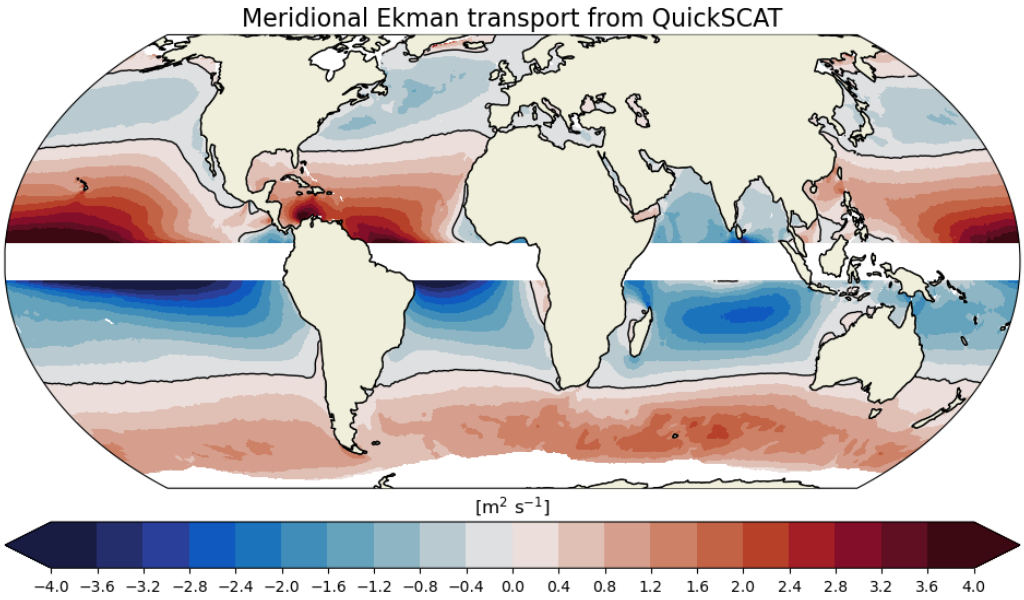

Figure 5.2: *Meridional Ekman volume transport, -$\tau^x / (f\rho_0)$, from QuickSCAT.*

We now define the ageostrophic mass transport in the Ekman layer as

$$\mathbf{M}_E = \int_{Ek} \rho_0 \mathbf{u_E} \, dz. \tag{5.21}$$

For a bottom Ekman layer, stress at the top will be zero. For a top Ekman layer, stress at the bottom will be zero:

$$Top: \quad \mathbf{f} \times \mathbf{M}_E = \boldsymbol{\tau}_T \tag{5.22}$$

$$Bottom: \quad \mathbf{f} \times \mathbf{M}_E = -\boldsymbol{\tau}_B \tag{5.23}$$

which is equivalent to writing

$$\boxed{Top: \quad \mathbf{M}_E = -\frac{1}{f} \mathbf{k} \times \boldsymbol{\tau}_T} \tag{5.24}$$

$$\boxed{Bottom: \quad \mathbf{M}_E = \frac{1}{f} \mathbf{k} \times \boldsymbol{\tau}_B.} \tag{5.25}$$

Take a situation in which $\tau_x = 0$ and therefore $M_{yE} = \int_{Ek} \rho_0 v_E \, dz = 0$ but $M_{xE} > 0$ with $\tau^y > 0$. **The net transport is thus at right angles to the stress at the surface (to the right for $f > 0$), and proportional to the magnitude of the stress.**

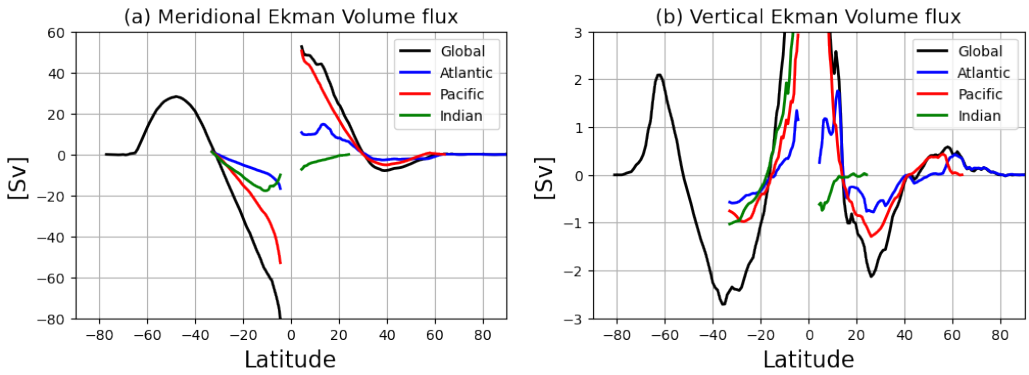

Figure 5.3: *(a) Meridional Ekman volume flux, -$\tau^x/(f\rho_0)$, for each of the world oceans as a function of latitude. Note the maximum of V_E at about 45°N and the changeover between westerlies and easterlies at about 30°N. (b) Vertical Ekman volume flux, w_e, for the world's oceans (see also Levitus, 1988).*

Integrated over the depth of the Ekman layer, the surface stress must be balanced by the Coriolis force, which in turn acts at right angles to the mass transport. **Mass transports in a top oceanic and bottom atmospheric Ekman layers are equal and opposite, because the stress is continuous across the ocean-atmosphere interface (see Fig.5.4).**

The Ekman vertical velocity: Ekman Pumping

We now obtain an expression for the vertical velocity induced by an Ekman layer. We start from the mass conservation equation

$$\frac{\partial u}{\partial x}+\frac{\partial v}{\partial y}+\frac{\partial w}{\partial z}=0 \tag{5.26}$$

and we integrate this over the Ekman layer

$$\int_{Ek}\left(\frac{\partial u}{\partial x}+\frac{\partial v}{\partial y}\right)\mathrm{d}z=-\int_{Ek}\frac{\partial w}{\partial z}\mathrm{d}z. \tag{5.27}$$

Remembering that we have defined $\mathbf{M}_E=\int_{Ek}\rho_0\mathbf{u_E}\,\mathrm{d}z$,

$$\frac{1}{\rho_0}\nabla\cdot\mathbf{M}_E = -\int_{Ek}\frac{\partial w}{\partial z}\mathrm{d}z \tag{5.28}$$

$$\frac{1}{\rho_0}\nabla\cdot\mathbf{M}_E = -(w_T-w_B). \tag{5.29}$$

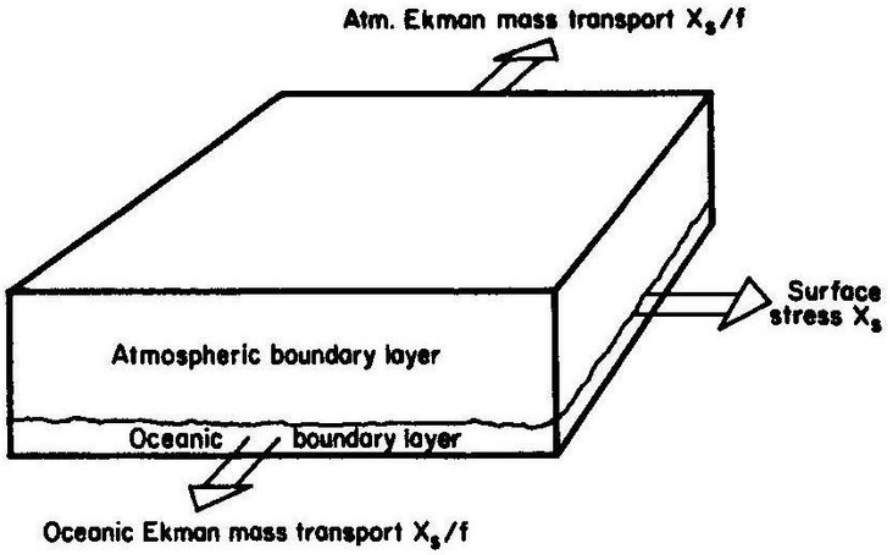

Figure 5.4: *The directions, for the northern hemisphere, and magnitude of the steady Ekman mass transports in the atmosphere and oceanic boundary layers when stress at the surface has the direction shown. Note that the sum of the atmospheric and oceanic Ekman mass transports is zero. When there is no pressure gradient, the force per unit area exerted by the surface stress on each boundary layer is equal to the product of mass per unit area and the Coriolis acceleration of the layer. The latter quantity is f times the Ekman mass transport and is directed at right angles to the stress. [from Gill (1982)]*

Using Eq.5.20:

$$\mathbf{f} \times \mathbf{M}_E = \boldsymbol{\tau}_T - \boldsymbol{\tau}_B, \tag{5.30}$$

and taking its curl we find

$$\nabla \cdot \mathbf{M}_E = \mathrm{curl}_z[(\boldsymbol{\tau}_T - \boldsymbol{\tau}_B)/f] \tag{5.31}$$

where we have used the curl_z operator on a vector $\mathbf{A}$ defined as $\mathrm{curl}_z\mathbf{A} \equiv \partial_x A_y - \partial_y A_x$.

We now make use of Eq.5.29 and we obtain

$$\frac{1}{\rho_0} \nabla \cdot \mathbf{M}_E = -(w_T - w_B) = \frac{1}{\rho_0} \mathrm{curl}_z[(\boldsymbol{\tau}_T - \boldsymbol{\tau}_B)/f]. \tag{5.32}$$

For a top Ekman layer we have:

$$\boxed{w_B = \frac{1}{\rho_0} \mathrm{curl}_z\Big(\boldsymbol{\tau}_T/f\Big)} \tag{5.33}$$

For a bottom Ekman layer we have:

$$\boxed{w_T = \frac{1}{\rho_0}\,\mathrm{curl}_z\left(\boldsymbol{\tau}_B / f\right)} \tag{5.34}$$

Friction induces a vertical velocity in the Ekman layer, proportional to the curl of the stress at the surface. This vertical velocity is called *Ekman pumping* (see Fig.5.3). The production of a vertical velocity at the edge of the Ekman layer is one of the most important effects of the layer, especially with regard to the large-scale circulation, for it provides an efficient means whereby surface fluxes are communicated to the interior flow.

5.3 A bottom boundary layer

We now derive the properties for the bottom boundary layer. If you are more atmospherically inclined, think of this bottom boundary layer as the one generated by the wind over some topography.

Our momentum equations (Eq.5.10) are completed by the mass conservation equation

$$\frac{\partial u}{\partial x} + \frac{\partial v}{\partial y} + \frac{\partial w}{\partial z} = 0 \tag{5.35}$$

and hydrostatic balance in the vertical

$$0 = -\frac{1}{\rho_0}\frac{\partial p}{\partial z}. \tag{5.36}$$

Remember we are in a Boussinesq fluid. The flow can be divided into an interior geostrophic part

$$-f v_g = -\frac{1}{\rho_0}\frac{\partial p}{\partial x} \tag{5.37}$$

$$f u_g = -\frac{1}{\rho_0}\frac{\partial p}{\partial y}, \tag{5.38}$$

$$\tag{5.39}$$

or

$$f(u_g, v_g) = (-\frac{\partial \phi}{\partial y}, \frac{\partial \phi}{\partial x}) \tag{5.40}$$

where $\phi \equiv p/\rho_0$. And a boundary layer correction

$$-fv = -\frac{1}{\rho_0}\frac{\partial p}{\partial x} + A\frac{\partial^2 u}{\partial z^2} \tag{5.41}$$

$$fu = -\frac{1}{\rho_0}\frac{\partial p}{\partial y} + A\frac{\partial^2 v}{\partial z^2}. \tag{5.42}$$

$$\tag{5.43}$$

Given Eq.5.40, the frictional-geostrophic balance can be written as

$$-f(v - v_g) = A\frac{\partial^2 u}{\partial z^2} \tag{5.44}$$

$$f(u - u_g) = A\frac{\partial^2 v}{\partial z^2}, \tag{5.45}$$

or even better as

$$\mathbf{f} \times (\mathbf{u} - \mathbf{u_g}) = A\frac{\partial^2 \mathbf{u}}{\partial z^2}. \tag{5.46}$$

Our boundary conditions will be

$$\text{at z=0:} \quad u = 0, v = 0 \quad \text{(no slip boundary condition)} \tag{5.47}$$

$$\text{as z}\rightarrow\infty\text{:} \quad u = u_g, v = v_g \quad \text{(a geostrophic interior).} \tag{5.48}$$

We seek solutions of the form

$$u = u_g + A_0 e^{\alpha z}, \quad v = v_g + B_0 e^{\alpha z}, \tag{5.49}$$

where A_0 and B_0 are constants. Substituting into Eq.5.46 leads to

$$fA_0 - AB_0\alpha^2 = 0, \quad -fB_0 - AA_0\alpha^2 = 0. \tag{5.50}$$

Remember that, given the absence of temperature horizontal gradients, via thermal wind, $\partial_z u_g = \partial_z v_g = 0$.

For non-trivial solutions we have $\alpha^4 = -f^2/A^2$, from which we find $\alpha = \pm(1 \pm i)(1/d)$, where $d = (2A/f)^{1/2}$. Using the boundary conditions we obtain the solution

$$u = u_g - e^{-z/d}\Big[u_g cos(z/d) + v_g sin(z/d)\Big] \tag{5.51}$$

$$v = v_g + e^{-z/d}\Big[u_g sin(z/d) - v_g cos(z/d)\Big]. \tag{5.52}$$

We have used $d = (2A/f)^{1/2}$, the depth of the Ekman layer. It is apparent that the solution decays exponentially from the surface with an e-folding scale equal to d.

Now let's suppose a flow that is directed eastward and has zero meridional component ($u_g > 0$, $v_g = 0$). Velocities reduce to

$$u = u_g[1 - e^{-z/d}cos(z/d)] \tag{5.53}$$
$$v = u_g \quad e^{-z/d}sin(z/d). \tag{5.54}$$

This is already telling us that the meridional velocity within the boundary layer is not zero. As $z \to 0$[1] we have

$$u = u_g[1 - (1 - z/d)] = u_g z/d \tag{5.55}$$
$$v = u_g \quad (1 - z/d)z/d = u_g z/d - \cancelto{0}{u_g z^2/d^2}. \tag{5.56}$$

Hence, u and v are equal and generate a flow that is 45° to the left of the direction of the interior flow (to the right when $f < 0$).

We can find a local maximum for the velocity in the boundary layer

$$\frac{\partial u}{\partial z} = 0 \to \partial_z[u_g - u_g e^{-z/d}cos(z/d)] = 0 \tag{5.57}$$

$$\frac{1}{d}u_g e^{-z/d}cos(z/d) + \frac{1}{d}u_g e^{-z/d}sin(z/d) = 0$$
$$cos(z/d) + sin(z/d) = 0$$
$$tan(z/d) = -1$$

And so the depth of maximum velocity is

$$z = \frac{3\pi}{4}d.$$

At this depth

$$u = u_g\Big(1 - e^{\frac{3\pi}{4}}cos(\frac{3\pi}{4})\Big) = 1.07u_g. \tag{5.58}$$

Hence, the theoretical value of u reaches values larger then the interior geostrophic flow because of frictional effects and redistribution of momentum within the boundary layer.

The bottom Ekman layer can be seen in Fig.5.5, where the Ekman spiral is depicted. At the bottom, the flow is at 45° to the left of the interior geostrophic flow. The maximum u is obtained at $z/d = \frac{3\pi}{4}$

[1]Taylor expanding and neglecting higher order terms $e^{-z/d} = 1 - z/d + \cancel{z^2/(2d^2)}$; $cos(z/d) = 1 - \cancel{z^2/(2d^2)}$; $sin(z/d) = z/d - \cancel{z^3/(3d^3)}$

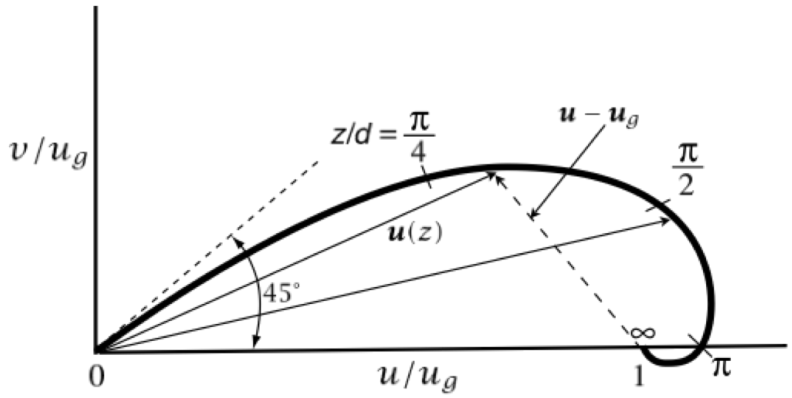

Figure 5.5: *The idealized Ekman layer solution at the bottom for $v_g = 0$. [from Vallis (2006)]*

Transport and vertical velocity

We now find an expression for the (cross-isobaric) transport produced by frictional effects. For $v_g = 0$, we have

$$V = \int_0^\infty v \, \mathrm{d}z = \int_0^\infty u_g e^{-z/d} sin(z/d) \, \mathrm{d}z = \frac{d}{2} u_g \quad (5.59)$$

$$U = \int_0^\infty (u - u_g) \, \mathrm{d}z = -\int_0^\infty u_g e^{-z/d} sin(z/d) \, \mathrm{d}z = -\frac{d}{2} u_g, \quad (5.60)$$

and the general case with $v_g \neq 0$ is simply

$$V = \frac{d}{2}(u_g - v_g) \quad (5.61)$$

$$U = -\frac{d}{2}(u_g + v_g). \quad (5.62)$$

The total mass transport caused by frictional forces is thus

$$\mathbf{M}_E = \frac{\rho_0 d}{2}\Big[-\mathbf{i}(u_g + v_g) + \mathbf{j}(u_g - v_g)\Big]. \quad (5.63)$$

Recalling that the frictionally induced transport in the Ekman layer is related to the stress at the surface by $\mathbf{M}_E = (\mathbf{k} \times \boldsymbol{\tau}_B)/f$, a full picture of stress, cross-isobaric velocity and total transport is given in Fig.5.6.

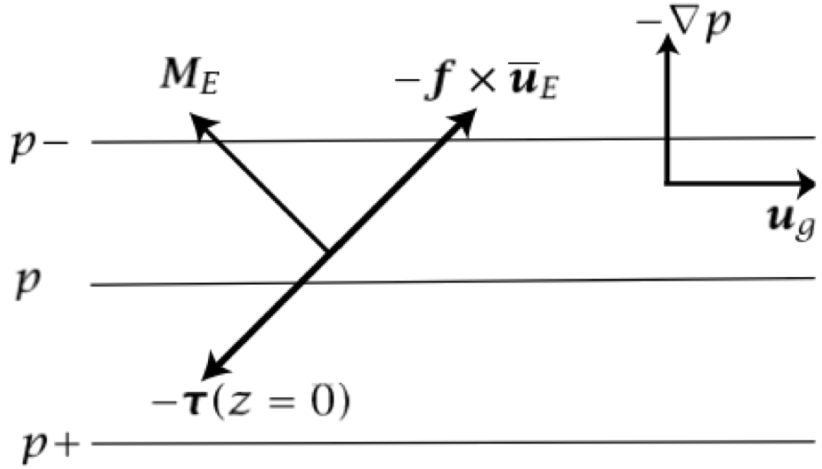

Figure 5.6: *A bottom Ekman layer, generated from an eastward geostrophic flow above. An overbar denotes a vertical integral over the Ekman layer. so that* $-f \times \overline{u}_E$ *is the Coriolis force on the vertically integrated Ekman velocity.* $\mathbf{M}_E$ *is the frictionally induced boundary layer transport, and* $\boldsymbol{\tau}$ *is the stress. [from Vallis (2006)]*

The flow within the Ekman layer has a nonzero divergence, indeed:

$$\frac{\partial U}{\partial x} + \frac{\partial V}{\partial y} = -\frac{d}{2}\Big[\partial_x(u_g + v_g) - \partial_y(u_g - v_g)\Big] \tag{5.64}$$

$$= \frac{d}{2}\Big[-(\partial_x u_g + \partial_y v_g) - \partial_x v_g + \partial_y u_g\Big]. \tag{5.65}$$

The first term on the r.h.s. is zero because the interior flow is non-divergent, hence:

$$\frac{\partial U}{\partial x} + \frac{\partial V}{\partial y} = -\frac{d}{2}(\partial_x v_g - \partial_y u_g) = -\frac{d}{2}\zeta_g \tag{5.66}$$

The vertical velocity at the top of the Ekman layer is, for a constant f (and using Eq.5.34)

$$\boxed{w_E = -\frac{1}{\rho_0}\nabla \cdot \boldsymbol{M}_E = \frac{1}{\rho_0}\,\mathrm{curl}_z\Big(\boldsymbol{\tau}_B/f\Big) = \frac{d}{2}\zeta_g} \tag{5.67}$$

There will be divergence if the interior geostrophic flow presents vorticity. **The vertical velocity at the top of the bottom Ekman layer, which**

arises because of the frictionally-induced divergence of the flow in the Ekman layer, is proportional to the geostrophic vorticity and to the Ekman layer height.

5.4 A surface boundary layer

We now look for solutions for a surface Ekman layer. In this case, the wind provides a stress on the upper ocean, and the Ekman layer serves to communicate this to the ocean interior.

We start again with our momentum equations, which for the interior geostrophic flow are

$$-fv_g = -\frac{1}{\rho_0}\frac{\partial p}{\partial x} \tag{5.68}$$

$$fu_g = -\frac{1}{\rho_0}\frac{\partial p}{\partial y}, \tag{5.69}$$

or

$$f(u_g, v_g) = (-\frac{\partial \phi}{\partial y}, \frac{\partial \phi}{\partial x}) \tag{5.70}$$

where $\phi \equiv p/\rho_0$. And for the Ekman layer

$$-fv = -\frac{1}{\rho_0}\frac{\partial p}{\partial x} + A\frac{\partial^2 u}{\partial z^2} \tag{5.71}$$

$$fu = -\frac{1}{\rho_0}\frac{\partial p}{\partial y} + A\frac{\partial^2 v}{\partial z^2}. \tag{5.72}$$

$$\tag{5.73}$$

The frictional-geostrophic balance can be written again as

$$-f(v - v_g) = A\frac{\partial^2 u}{\partial z^2} \tag{5.74}$$

$$f(u - u_g) = A\frac{\partial^2 v}{\partial z^2}, \tag{5.75}$$

or even better as

$$\boxed{\mathbf{f} \times (\mathbf{u} - \mathbf{u_g}) = A\frac{\partial^2 \mathbf{u}}{\partial z^2}} \tag{5.76}$$

Our boundary conditions will be

$$\text{at z=0:} \qquad \tau^x = \rho_0 A \frac{\partial^2 u}{\partial z^2}, \text{ (a given surface stress)} \tag{5.77}$$

$$\tau^y = \rho_0 A \frac{\partial^2 v}{\partial z^2} \tag{5.78}$$

$$\text{as z}\rightarrow -\infty: \qquad u = u_g \text{ (a geostrophic interior)} \tag{5.79}$$

$$v = v_g \tag{5.80}$$

We now introduce the kinematic wind stress at the surface, $\tilde{\boldsymbol{\tau}} = \boldsymbol{\tau}/\rho_0$, and seek solutions by the same method we used for the bottom layer:

$$u = u_g + \frac{\sqrt{2}}{fd} e^{z/d} \Big[\tilde{\tau}^x cos(z/d - \pi/4) - \tilde{\tau}^y sin(z/d - \pi/4) \Big], \tag{5.81}$$

$$v = v_g + \frac{\sqrt{2}}{fd} e^{z/d} \Big[\tilde{\tau}^x sin(z/d - \pi/4) + \tilde{\tau}^y cos(z/d - \pi/4) \Big]. \tag{5.82}$$

Note that the boundary layer correction depends only on the imposed surface stress, and not on the interior flow. In the absence of an imposed stress the boundary layer correction is zero, and $\mathbf{u} = \mathbf{u}_g$. Similar to the bottom boundary layer, the velocity vector traces a diminishing spiral as it descend into the interior (Fig.5.7). The velocity within the boundary depends on its depth, $d = \sqrt{\frac{2A}{f}}$, which depends on the eddy viscosity A. If the fluid is not very viscous, it will generate a small Ekman layer, and the velocity within the layer can be large for small stresses.

What is the value and direction of the surface velocity? at $z = 0$ we have

$$u(0) = u_g + \frac{\sqrt{2}}{fd} \Big[\tilde{\tau}^x cos(-\pi/4) - \tilde{\tau}^y sin(-\pi/4) \Big], \tag{5.83}$$

$$v(0) = v_g + \frac{\sqrt{2}}{fd} \Big[\tilde{\tau}^x sin(-\pi/4) + \tilde{\tau}^y cos(-\pi/4) \Big]. \tag{5.84}$$

Since $cos(-\pi/4) = \sqrt{2}/2$ and $sin(-\pi/4) = -\sqrt{2}/2$, the solution is

$$u(0) = u_g + \frac{\sqrt{2}}{fd} \Big[\tilde{\tau}^x \frac{\sqrt{2}}{2} + \tilde{\tau}^y \frac{\sqrt{2}}{2} \Big], \tag{5.85}$$

$$v(0) = v_g + \frac{\sqrt{2}}{fd} \Big[- \tilde{\tau}^x \frac{\sqrt{2}}{2} + \tilde{\tau}^y \frac{\sqrt{2}}{2} \Big]. \tag{5.86}$$

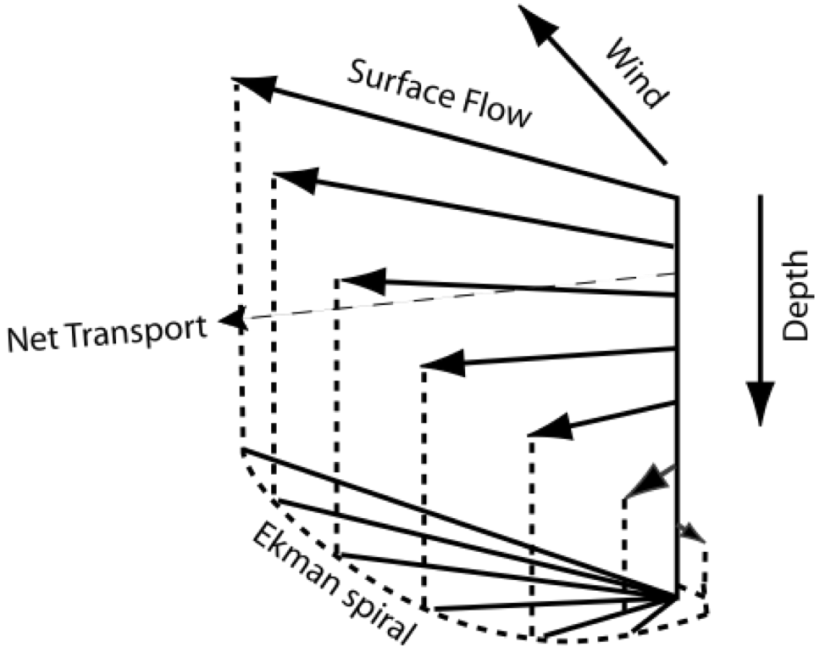

Figure 5.7: *An idealized Ekman spiral in the southern hemisphere ocean, driven by an imposed wind stress. The net transport is at right angles to the wind, independent of the detailed form of the friction. The angle of the surface flow is at 45° to the wind (only for a Newtonian viscosity). [from Vallis (2006)]*

Suppose the surface wind is eastward. In this case $\tilde{\tau}^y = 0$ and the solutions reduce to

$$u(0) = u_g + \frac{\sqrt{2}}{fd}\left[\tilde{\tau}^x \frac{\sqrt{2}}{2}\right], \tag{5.87}$$

$$v(0) = v_g - \frac{\sqrt{2}}{fd}\left[\tilde{\tau}^x \frac{\sqrt{2}}{2}\right]. \tag{5.88}$$

The velocity at the surface of the Ekman layer are simply

$$u(0) - u_g = \frac{\tilde{\tau}^x}{fd'} \tag{5.89}$$

$$v(0) - v_g = -\frac{\tilde{\tau}^x}{fd}. \tag{5.90}$$

Therefore the magnitudes of the frictional flow in the x and y directions are equal to each other, and the ageostrophic flow is 45° to the right (for $f > 0$**) of the wind.** This result does not depend on the size of the viscosity.

Transport and vertical velocity (or Ekman pumping / suction)

The transport induced by the surface stress is obtained by integrating (5.81) and (5.82)

$$U = \int_{-\infty}^{0} (u - u_g)\,\mathrm{d}z = \frac{\tilde{\tau}^y}{f} \tag{5.91}$$

$$V = \int_{-\infty}^{0} (v - v_g)\,\mathrm{d}z = -\frac{\tilde{\tau}^x}{f}, \tag{5.92}$$

which indicates that **the ageostrophic transport is perpendicular to the wind stress**, as previously noted (see Fig.5.8). It should be noted that these results are correct even if the details of the Ekman spiral are not.

Again the ageostrophic flow will be divergent

$$\frac{\partial U}{\partial x} + \frac{\partial V}{\partial y} = \int_{-\infty}^{0} \mathrm{d}z \left(\frac{\partial U}{\partial x} + \frac{\partial V}{\partial y} \right) = \frac{1}{f} \left(\partial_x \tilde{\tau}^y - \partial_y \tilde{\tau}^x \right) = \tag{5.93}$$

$$w_E = \frac{1}{f} \mathrm{curl}_z \tilde{\boldsymbol{\tau}}. \tag{5.94}$$

As previously noted in (5.33). At the edge of the Ekman layer the vertical velocity (*Ekman pumping*) is proportional to the curl of the wind stress.

The Ekman pumping is associated with the frictionally induced vertical velocity w_E. This vertical Ekman velocity starts with zero due to

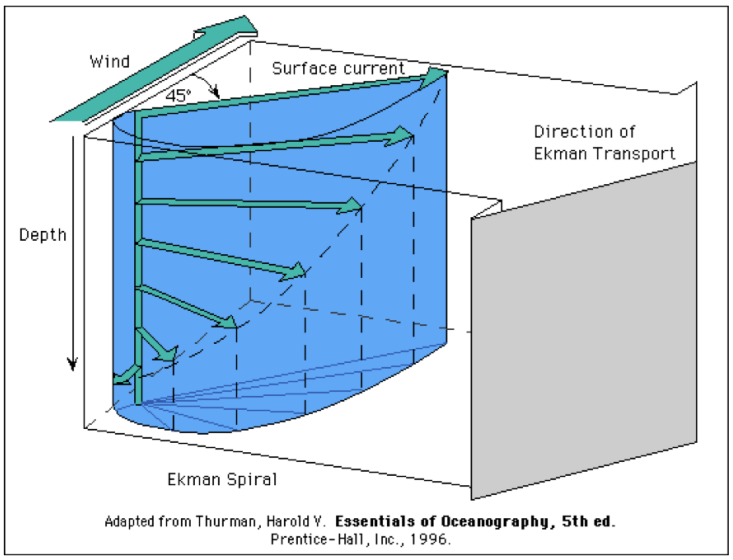

Figure 5.8: An idealized Ekman velocity spiral.

the boundary condition at the surface, followed by an exponential pattern within the top Ekman layer, and approaches a constant below.

It is quite hard to observe Ekman spirals both in the ocean and atmosphere (but not in a laboratory where you can control viscosity and background conditions!). The theory does not take into account stratification, gravity waves and assumes a steady wind. Nevertheless both the Ekman mass transport and vertical velocity are independent of details of the Ekman layer, and only depend on the imposed stress (Fig. 5.9 and Fig. 5.11).

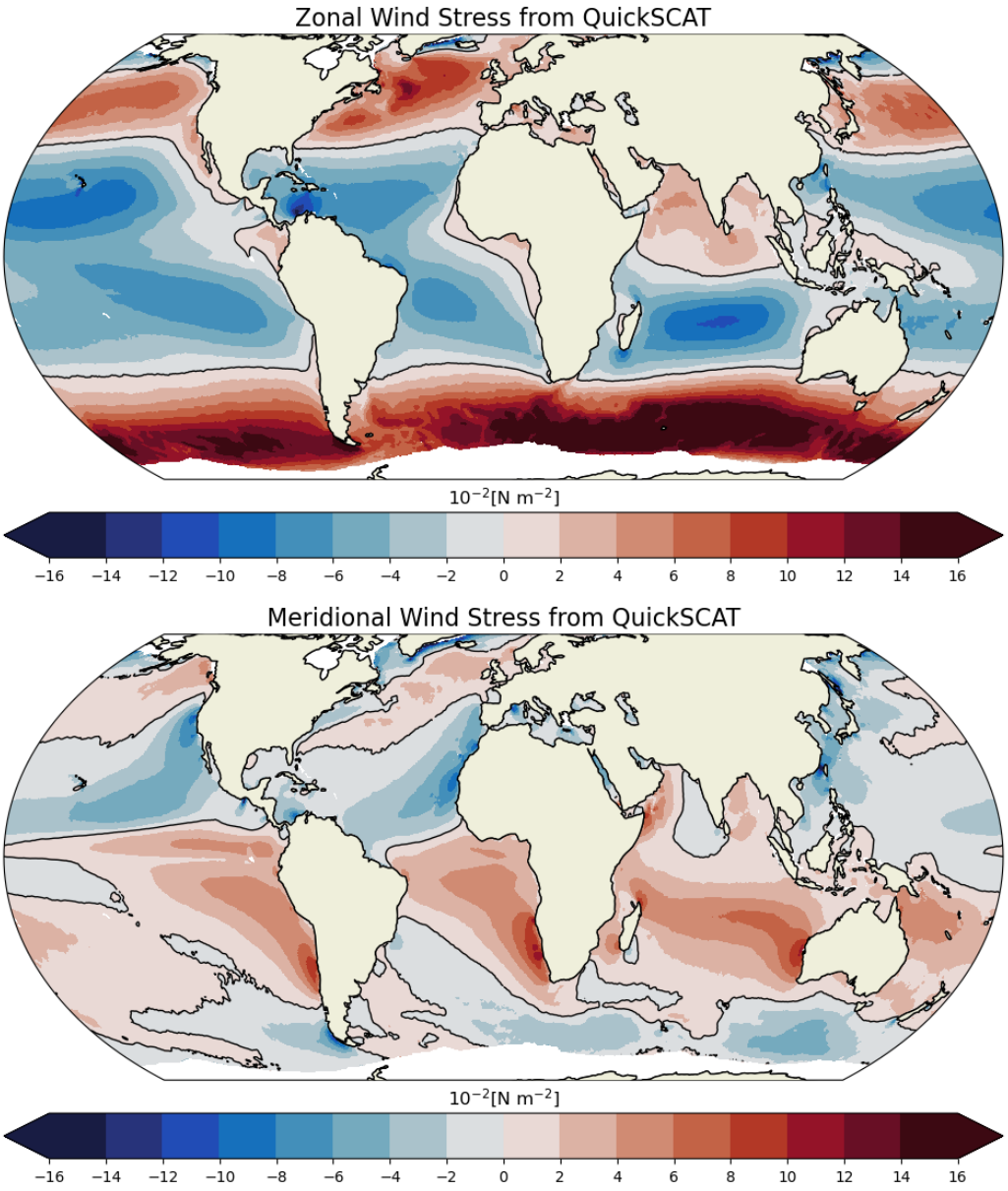

Figure 5.9: *Climatological zonal and meridional wind stress from QuickSCAT.*

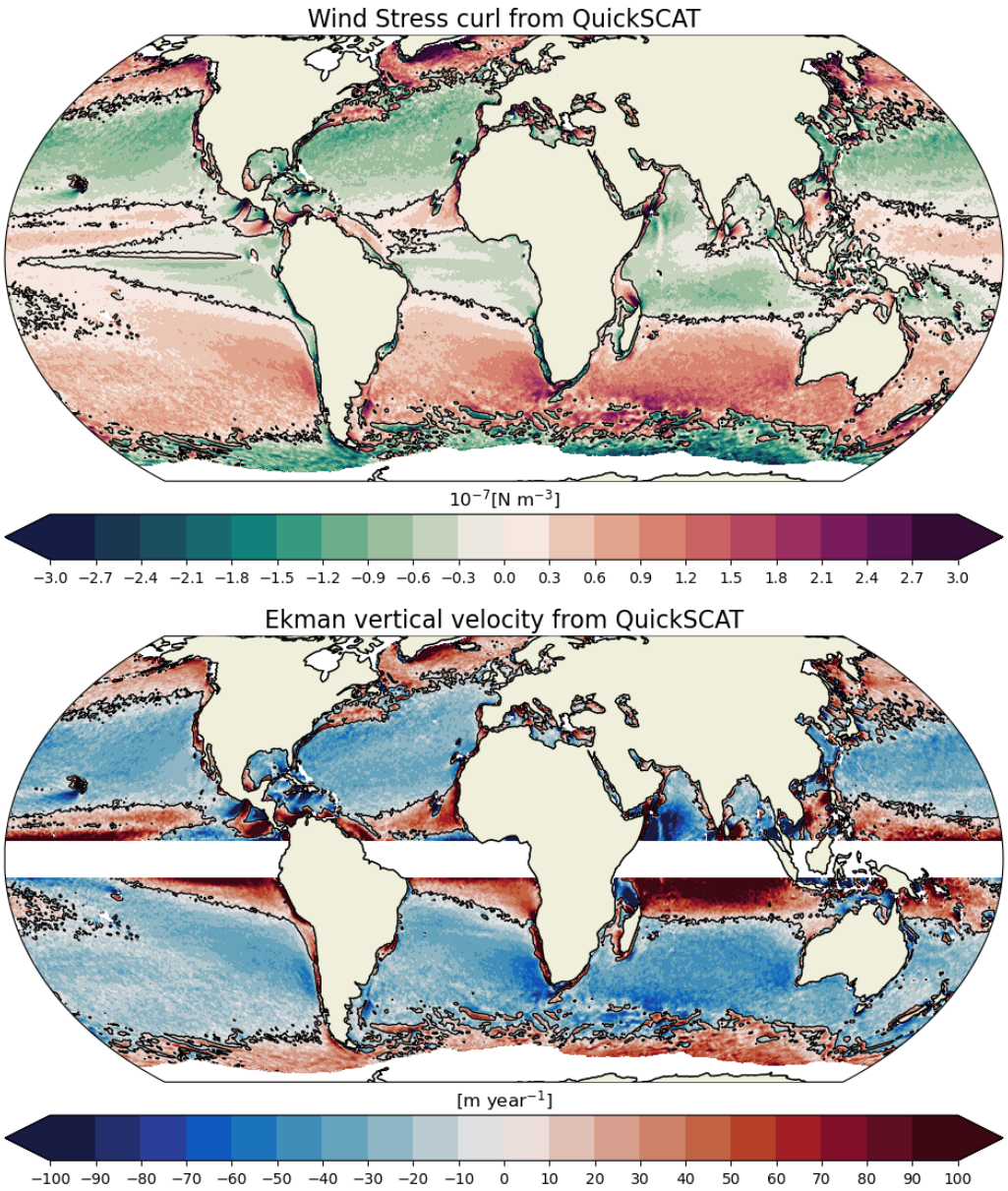

Figure 5.10: *Climatological wind stress curl and Ekman pumping velocity, w_e (m/year), from QuickSCAT. It is positive in the subtropical regions on the order of 20-50 m per year and mostly negative over the subpolar regions. Towards the equator, f goes to zero, and Ekman pumping and Ekman transport become ill-defined.*

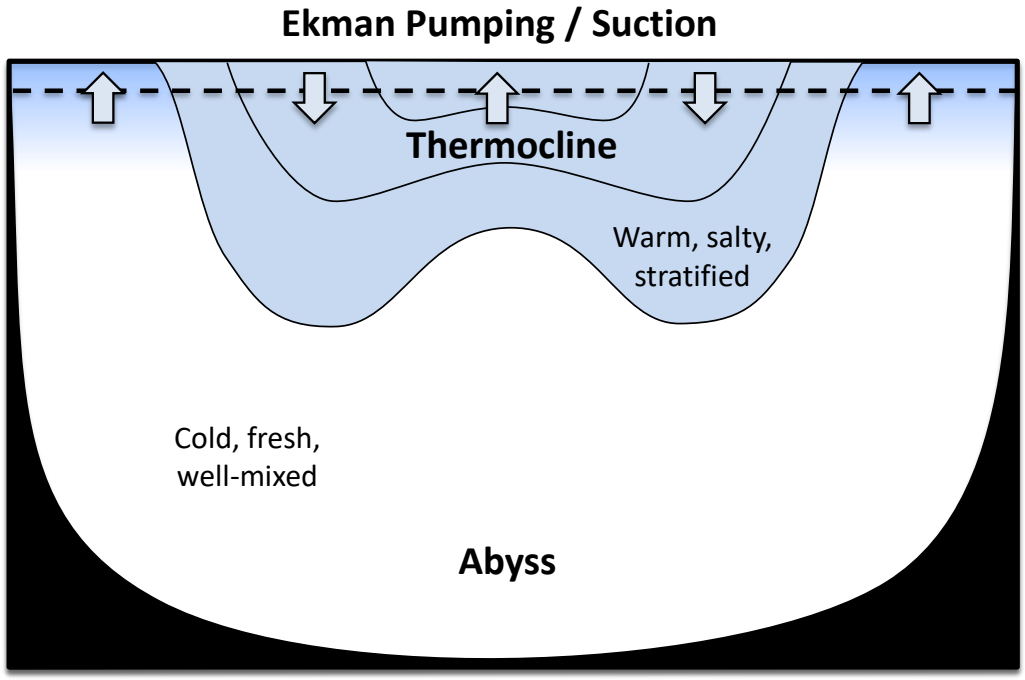

Figure 5.11: *The direction of Ekman pumping and suction is responsible for the odd bi-modal shape of the ocean's density anomaly.*

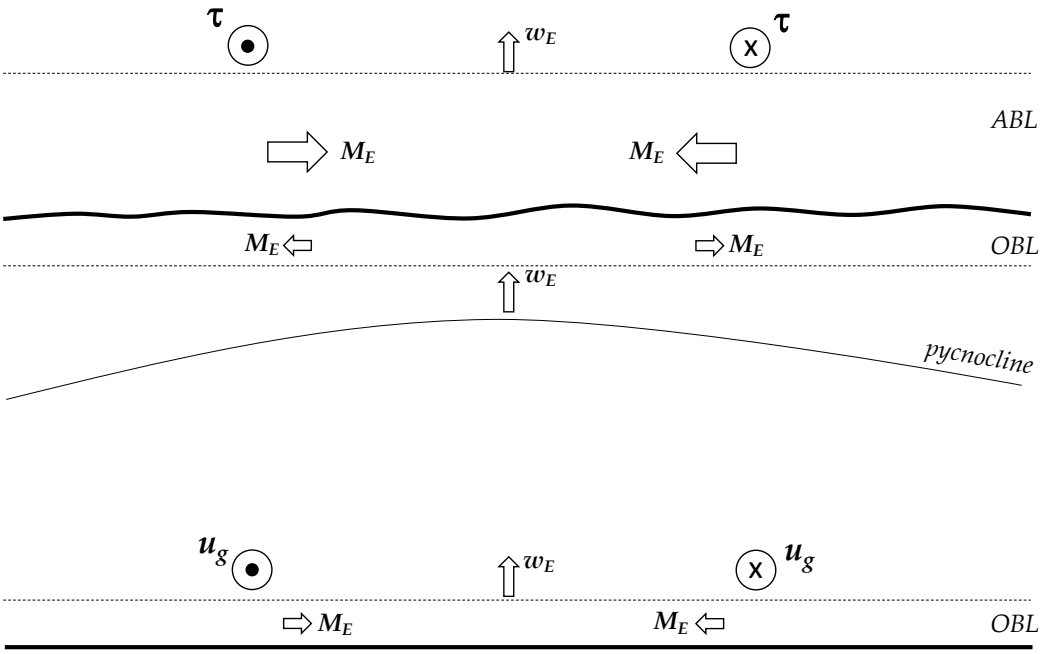

Figure 5.12: *Section through a cyclonic wind over the ocean. The geostrophic wind gives a cyclonic rotation around the low-pressure center. The Ekman mass transport in the atmospheric boundary layer is inward, bringing mass to fill the low, and the associated vertical pumping velocity is therefore upward. The Ekman mass transport in the oceanic boundary layer is equal and opposite to that in the atmosphere, so there is an outward mass transport and upward pumping velocity in the ocean. This tends to raise the thermocline. The upper Ekman layer in the ocean is primarily driven by an imposed wind stress, whereas the lower Ekman layer in the ocean largely results from the interaction of interior geostrophic velocity and a rigid lower surface [from Vallis (2006) and Gill (1982)].*

Ekman velocity Spiral

- Frictionally induced surface velocity to the right of the wind (for $f > 0$, due to Coriolis)
- Surface layer pushes next layer down slightly to the right, generating a slightly weaker current
- Next layer pushes next layer, slightly to right and generating a slightly weaker current
- Producing a "spiral" of the current vectors, to the right in the northern hemisphere, with decreasing speed as depth increases
- Details of the spiral depend on the vertical viscosity (how frictional the flow is, and also whether friction depends on depth)
- The total transport only depends on the imposed wind stress
- Typical transport size: for a wind stress 0.1 N m^{-2}, $M_E = \tau/(\rho f)$ =1 m^2 s^{-1}. Integrate this over 'width' of the ocean, say 5000 km, we get a total transport of 5×10^6 m^3 s^{-1}= 5 Sv (1 $Sv \equiv 10^6$ m^3 s^{-1})

5.5 Upwelling

5.5.1 Coastal Upwelling

Suppose we have a wind which is entirely meridional, $\tau^x = 0$, and therefore $M_E^y = 0$ and $M_E^x > 0$ for $\tau^y > 0$. The net transport will be to the left of and at right angles to the wind direction (for $f < 0$). Continuity requires that there must be inflow from the right of the wind direction. If the wind is blowing parallel to a coastline which is on the right of the wind, as the wind causes an Ekman frictionally induced transport to the left away from the coast, water is replaced from below, generating a so-called *coastal upwelling* near the region of divergence along the coast.

Coastal upwelling is accompanied by a rise in upper ocean isopycnals toward the coast. This creates an equatorward geostrophic surface flow, the *eastern boundary current*. Poleward undercurrents are observed at about 200 m depth beneath the equatorward surface currents (Fig.5.13c). Poleward undercurrents are created mainly by the alongshore pressure gradient that drives the onshore subsurface geostrophic flow that feeds the upwelling.

Given the prevailing wind directions, the largest coastal upwelling regions happen to be on eastern boundaries of ocean basins. Eastern boundary upwelling systems (EBUS) cover less than 3% of the world ocean surface yet they have a significant role in the climate system, and are home to the largest contribution of ocean biological productivity with up to 40% of the reported global fish catch (Fig.5.14). The upwelled water does not come from great depths. Observations and models show that upwelled water comes from depths not greater than 200-300 m. Usually the upwelled water has high nutrient content, and plankton production may be promoted with important biological consequences when photosynthesis is activated in the photic zone.

Coupled with the vast coastal human populations, these regions play key biological and socio-economical roles. There are common features to eastern boundary upwelling regions: wind-driven flows, alongshore currents, steep shelves and large vertical and offshore nutrient transports. Despite the commonality, each of the main upwelling systems (California, Humboldt, Canary and Benguela Current Systems), exhibits substantial differences in primary productivity, phytoplankton biomass, and community structures. The reasons for these differences are not fully understood.

Many coupled climate models generate very large sea surface temperature (SST) biases in the coastal upwelling regions of the California Current System, the Humboldt Current system and the Benguela Current System,

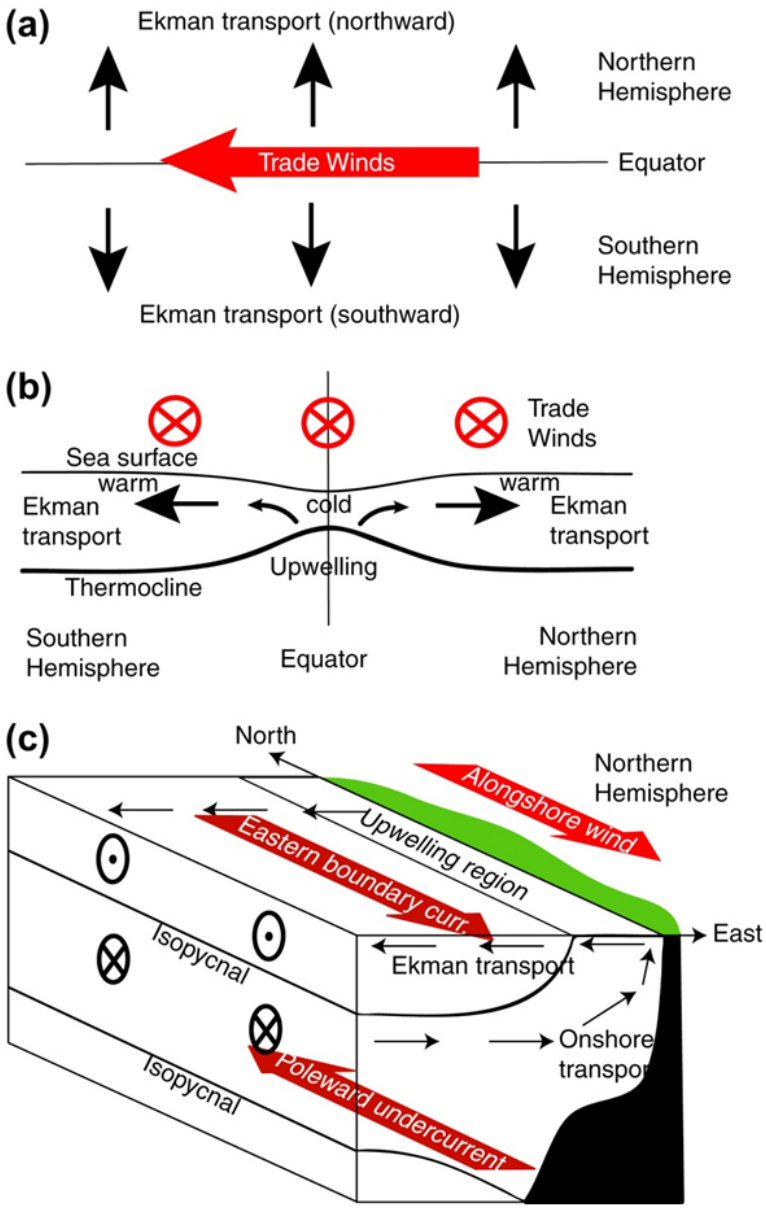

Figure 5.13: *Ekman transport divergence near the equator driven by easterly trade winds. (a) Ekman transports. (b) Meridional cross-section showing effect on the thermocline and surface temperature. (c) Coastal upwelling system due to an alongshore wind with offshore Ekman transport ($f > 0$). The accompanying isopycnal deformations and equatorward eastern boundary current and poleward undercurrent are also shown. [from Talley et al. (2011)]*

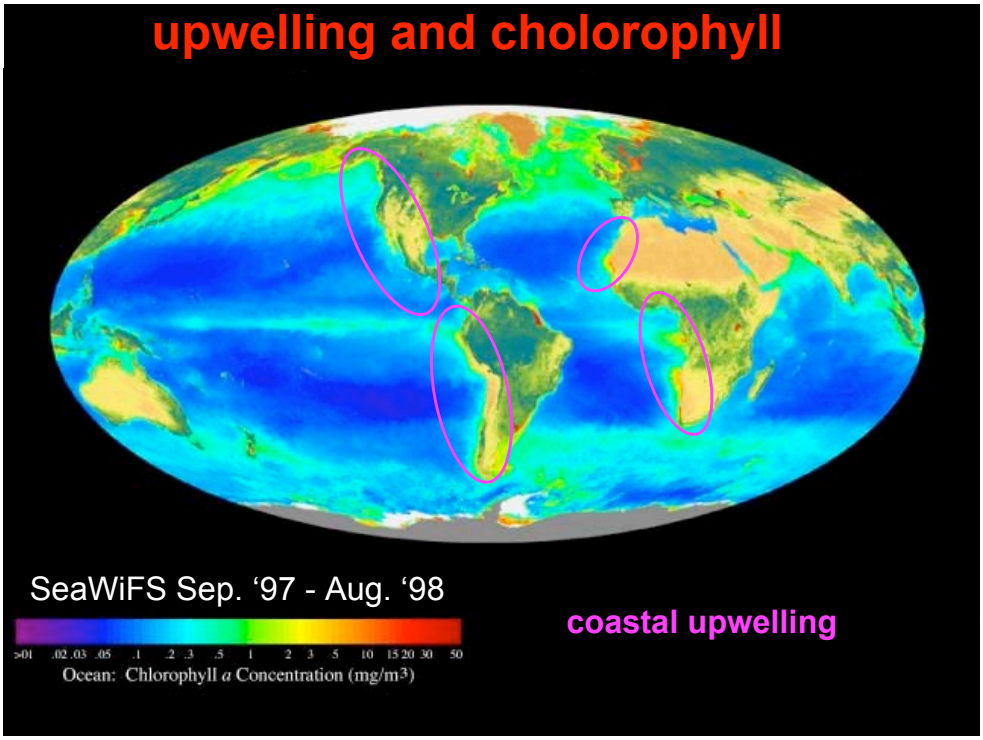

Figure 5.14: *A false-color image depicting chlorophyll-a concentration as measured from the SeaWIFS satellite data. Eastern Boundary Upwelling systems (EBUS) regions (California, Peru, Canary and Benguela) are shown by the pink ovals.*

where simulated mean SSTs are much warmer than observed (typically in excess of 3°C and as high as 10°C; see Fig.5.15). Furthermore, these SST biases have significant remote effects on surface and subsurface temperature and salinity, and on precipitation and hence atmospheric heating and circulation. The warm temperature biases associated with upwelling regions strongly limit the prediction of future evolution of these regions. Increased model resolution, achieved via nesting or adaptive gridding, improves simulations of the regional climate and affects the large-scale climate system through feedbacks.

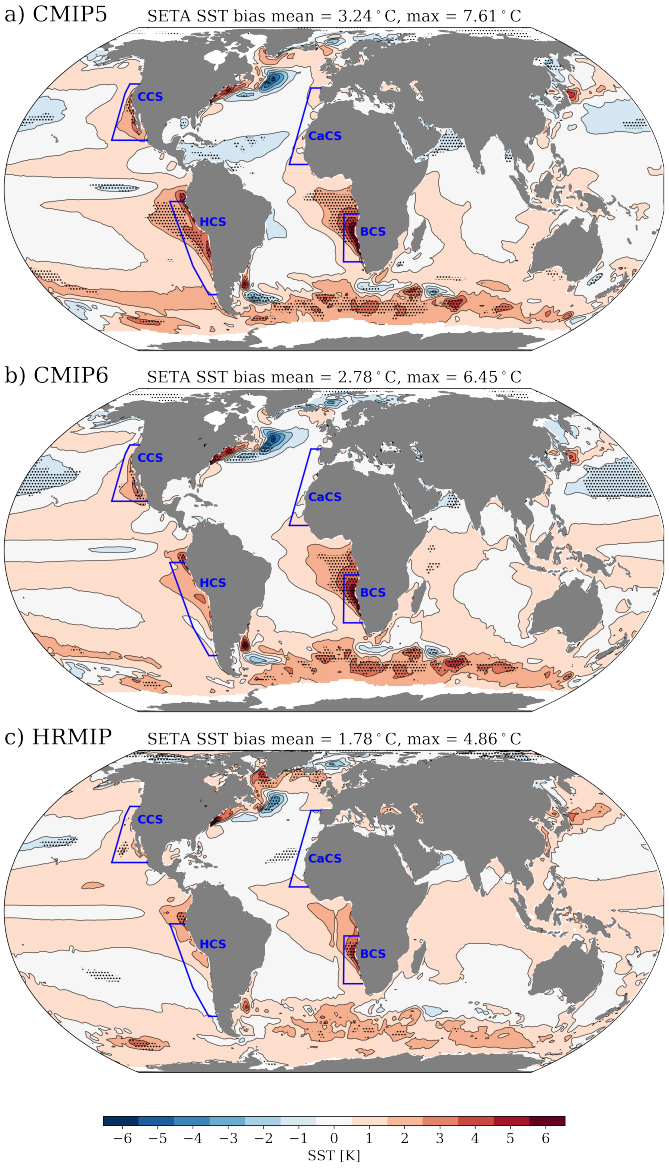

Figure 5.15: *Time-mean (1985-2004) SST bias for (a) CMIP5, (b) CMIP6 and (c) HighResMIP multi-model mean relative to OISST. Every contour represents an SST bias of 1 K. Black dots show regions where all models agree on the sign of the bias. The poles are excluded in order to highlight the biases in the EBUS regions, which present the highest SST anomalies. The 4 major EBUS are: the California Current System (CCS), the Canary Current System (CaCS), the Humboldt Current system (HCS) and the Benguela Current System (BCS). [from Farneti et al. (2022)]*

5.5.2 Equatorial Upwelling

Equatorial upwelling due to Ekman transport results from the westward wind stress (trade winds). These cause northward Ekman transport north of the equator and southward Ekman transport south of the equator. This results in upwelling along the equator, even though the wind stress curl is small because of the Coriolis parameter dependence in (5.33).

At the equator, where the Coriolis parameter changes sign, zonal (east-west) winds can cause Ekman convergence or divergence even without any variation in the wind (Fig.5.13a). Right on the equator, there is no Ekman layer since the Coriolis force that would create it is zero ($f = 0$). If the equatorial wind is westward (a trade wind), then the Ekman transport just north of the equator is northward, and the Ekman transport just south of the equator is southward, and there must be upwelling into the surface layer on the equator.

Trade winds are relatively steady easterlies. They are driven by warm waters in the western region and cooler waters in the east, which creates rising air in the west and sinking air in the east, and a thermally direct flow from east to west to feed this (Walker cell). In the ocean the true equatorial region is much narrower - about 2 degrees wide. Easterly trade winds at the equator drive (1) poleward Ekman transport and (2) westward surface flow, as follows. The easterly trade winds cause northward Ekman transport just to the north of the equator and southward Ekman transport just to the south of the equator. This causes upwelling at the equator. As a result, the pycnocline shoals towards the equator (Fig.5.13b). **This drives a westward geostrophic flow at the sea surface.**

Directly on the equator, the effect of rotation on the circulation vanishes, and so the concepts of geostrophic and Ekman flow do not apply. At the equator, the easterly trade winds push the surface water directly (frictionally) from east to west. This water piles up gently in the western Pacific (0.5 meters higher there than in the eastern Pacific). The pycnocline is deeper in the west also as a result, and much warmer water is found there (so-called **"warm pool"**). Upwelling in the east draws cool water to the surface because of the shallow pycnocline there, but intense eastward-flowing upwelling in the west cannot create cold water at the surface there because of the thickness of the warm pool.

Because the sea surface is higher in the west than in the east, there is a pressure difference that causes the flow just beneath the surface layer to be eastward. This strong eastward flow is the Equatorial Undercurrent. It is centered at about 150 to 200 m depth. EUC speeds are in excess of 100 cm/sec. The current is exceptionally thin vertically (about 150 m

thick). The Equatorial Undercurrent shoals towards the east, as does the pycnocline. The shoaling is associated with upwelling of cool water in the central/eastern Pacific, giving rise to the ”cold tongue” (in non-El Niño years). Steady trade winds, which cause equatorial upwelling, are more prevalent in the east than in the west. When the trade winds weaken or even reverse, the flow of water westward at the equator weakens or reverses and upwelling weakens or stops. Surface waters in the eastern Pacific warm significantly since upwelling is no longer bringing the cool waters to the surface. The deep warm pool in the western Pacific thins as its water sloshes eastward along the equator in the absence of the trade winds which maintain it.

Exercices

1. For $A = 10^{-1}$ m^2 s^{-1} and $f = 10^{-4}\ s^{-1}$, what would be the typical depth of an Ekman layer?

2. Assume that the atmospheric Ekman layer over the earth's surface at latitude 45°N can be modeled with a turbulent kinematic viscosity $\nu = 10$m^2 s^{-1}. If the geostrophic velocity above the layer is 10 m s^{-1} and is uniform, what is the vertically integrated flow across the isobars (pressure contours)? Is there any vertical velocity?

3. Meteorological observations above New York City (41°N) reveal a neutral atmospheric boundary layer (no convection and no stratification) and a westerly geostrophic wind of 12 m s^{-1} at 1000 m above street level. Under neutral conditions, Ekman layer dynamics apply. Using an eddy viscosity of 10 m^2 s^{-1}, determine the wind speed and direction atop the World Trade Center (height: 411 m).

4. Between 15°N and 45°N, the winds over the North Pacific consist mostly of the easterly trades (15°N to 30°N) and the westerlies (30°N to 45°N. An adequate representation is

$$\tau^x = \tau_0 sin\Big(\frac{\pi y}{2L}\Big), \quad \tau^y = 0, \quad -L \leq y \leq L, \tag{5.95}$$

   where $\tau_0 = 0.15\ N/m^2$ is the maximum wind stress and $L = 1670\ km$. Taking $\rho_0 = 1028\ kg/m^3$ and the value of the Coriolis parameter corresponding to 30°N, calculate the Ekman pumping. Which way is it directed? Calculate the vertical volume flux over the entire 15°N-45°N strip of the North Pacific (width = 8700 km). Express your answer in Sverdrup units (1 Sverdrup = 1 Sv $\equiv 10^6$ m^3 s^{-1}).

Chapter 6

Wind-Driven Circulation

We will now use and integrate both Ekman theory and the geostrophic approximation to get a first solution to the wind-driven circulation. They will be the basis for the theory of the wind-driven gyres. At first, the theory will be simple, with no topography and in a steady state, but it will be able to explain many of the qualitative features of the wind-driven circulation.

The first theory presented is the steady, forced-dissipative, homogeneous model first formulated by Stommel; and different versions will be discussed.

We start with the simplest model that can capture our physical setting. We will assume (see Fig. 6.1)

- a homogeneous (or depth-integrated) model.
- Flat bottom.
- Steady state.
- The β-plane approximation.

Let's now remember the solutions for the top and bottom Ekman vertical velocities, and the momentum equations for the geostrophic flow:

$$w_E^T = \frac{1}{f_0}\left(\partial_x \tilde{\tau}^y - \partial_y \tilde{\tau}^x\right) = \frac{1}{f_0}\,\mathrm{curl}_z\,\tilde{\boldsymbol{\tau}}_T = \frac{1}{\rho_0 f_0}\mathrm{curl}_z\,\boldsymbol{\tau}_T \tag{6.1}$$

$$w_E^B = -\frac{1}{\rho_0}\,\nabla\cdot\boldsymbol{M}_E = \frac{1}{f_0}\,\mathrm{curl}_z\,\tilde{\boldsymbol{\tau}}_B = \frac{d}{2}\zeta_g, \tag{6.2}$$

where $\zeta_g = (\partial_x v_g - \partial_y u_g)$ is the vorticity of the interior geostrophic flow.

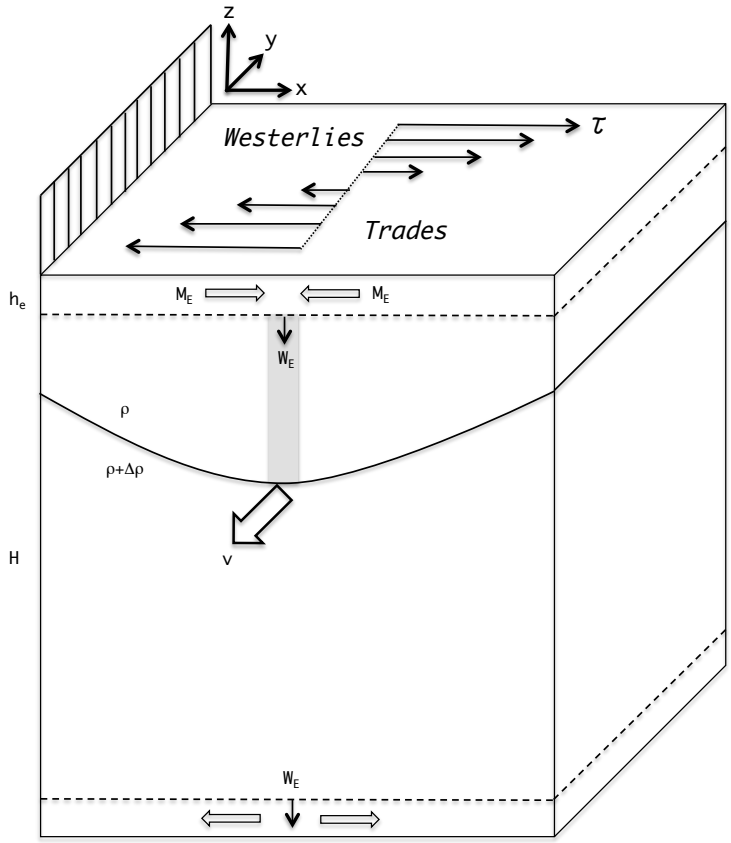

Figure 6.1: *A schematic of an idealized wind-driven Ekman pumping on a β-plane for a homogeneous ocean of depth H, resulting in a simple model for mid-latitude ocean circulation.*

The interior geostrophic flow (for a homogeneous barotropic fluid in which $\rho' = 0$) is

$$-fv = -\frac{1}{\rho_0}\frac{\partial p}{\partial x} \tag{6.3}$$

$$fu = -\frac{1}{\rho_0}\frac{\partial p}{\partial y} \tag{6.4}$$

$$0 = \frac{1}{\rho_0}\frac{\partial p}{\partial z} \tag{6.5}$$

$$\frac{\partial u}{\partial x} + \frac{\partial v}{\partial y} + \frac{\partial w}{\partial z} = 0 \tag{6.6}$$

6.1 A linear geostrophic vorticity balance approach: Sverdrup Balance

Within a β-plane, the interior geostrophic flow becomes

$$-(f_0 + \beta y)v = -\frac{1}{\rho_0}\frac{\partial p}{\partial x} \tag{6.7}$$

$$(f_0 + \beta y)u = -\frac{1}{\rho_0}\frac{\partial p}{\partial y} \tag{6.8}$$

$$0 = \frac{1}{\rho}\frac{\partial p}{\partial z} \tag{6.9}$$

$$\nabla_3 \cdot \boldsymbol{v} = 0. \tag{6.10}$$

And we will use $\boldsymbol{v} = (u, v, w)$ and $\boldsymbol{u} = (u, v)$.

Cross-differentiating the horizontal momentum equations [∂_x(6.8)-∂_y(6.7)] gives:

$$f_0\Big(\frac{\partial u}{\partial x} + \frac{\partial v}{\partial y}\Big) + \beta y\Big(\frac{\partial u}{\partial x} + \frac{\partial v}{\partial y}\Big) + \beta v = 0. \tag{6.11}$$

But since in a β-plane $\beta y \ll f_0$, we have

$$f_0\Big(\frac{\partial u}{\partial x} + \frac{\partial v}{\partial y}\Big) + \beta v = 0. \tag{6.12}$$

or

$$\boxed{\beta v = f_0\frac{\partial w}{\partial z}} \tag{6.13}$$

Which is a form of the linear geostrophic vorticity balance, and is known as **SVERDRUP BALANCE**.

Eq.6.13 expresses a conservation of potential vorticity. If $\frac{\partial w}{\partial z} > 0$, there will be stretching of the fluid column. *As the column stretches and shrinks it has to increase its vorticity in order to conserve angular momentum*. At large scales, the only significant vorticity is the planetary vorticity f, which in this case has to increase to balance the positive $\frac{\partial w}{\partial z}$. β is indeed a rate of vorticity change $\left(\frac{\partial f}{\partial y}\right)$. This balance is responsible for a meridional velocity v.

Geostrophy was previously studied on a f-plane, resulting in $w = 0$. We now find a vertical velocity within the geostrophic flow using the β-plane. If $\beta = 0 = \frac{\partial f}{\partial y}$, then the vertical geostrophic velocity is $w = 0$.

What is the structure of $\frac{\partial w}{\partial z}$?

Taking the vertical derivative of the horizontal momentum equations

$$-(f_0+\beta y)\frac{\partial v}{\partial z} = -\frac{1}{\rho_0}\frac{\partial^2 p}{\partial x \partial z} \tag{6.14}$$

$$(f_0+\beta y)\frac{\partial u}{\partial z} = -\frac{1}{\rho_0}\frac{\partial^2 p}{\partial y \partial z}. \tag{6.15}$$

But $\frac{\partial p}{\partial z} = 0$. Hence $\frac{\partial u}{\partial z} = \frac{\partial v}{\partial z} = 0$ and the flow is barotropic and there is no vertical shear. $\frac{\partial w}{\partial z}$ is constant throughout the interior and different from zero.

Now take a vertical derivative of the vertical velocity, and remembering the Ekman solutions we find

$$\frac{\partial w}{\partial z} = \frac{w_T - w_B}{H} = \frac{1}{\rho_0 f_0 H} curl_z \boldsymbol{\tau} - \frac{d}{2H}\zeta_g, \tag{6.16}$$

where H is the depth of the interior flow.

Using the geostrophic expressions for the horizontal velocities

$$-\frac{\partial v}{\partial x} = -\frac{1}{\rho_0 f_0}\frac{\partial^2 p}{\partial x^2} \tag{6.17}$$

$$\frac{\partial u}{\partial y} = -\frac{1}{\rho_0 f_0}\frac{\partial^2 p}{\partial y^2} \tag{6.18}$$

our solution $\beta v = f_0 \frac{\partial w}{\partial z}$ becomes

$$\frac{\beta}{\rho_0 f_0^2}\frac{\partial p}{\partial x} = \frac{1}{\rho_0 f_0 H} curl_z \boldsymbol{\tau} - \frac{d}{2H\rho_0 f_0}\Big(\frac{\partial^2 p}{\partial x^2} + \frac{\partial^2 p}{\partial y^2}\Big), \tag{6.19}$$

since $\zeta = (\frac{\partial v}{\partial x} - \frac{\partial u}{\partial y})$. Or

$$\underbrace{\beta\frac{\partial p}{\partial x}}_{\text{meridional velocity}} = \frac{f_0}{H}\Big(\underbrace{curl_z \boldsymbol{\tau}}_{\substack{\text{Ekman at}\\ \text{the top}}} - \underbrace{\frac{d}{2}\nabla^2 p}_{\substack{\text{Ekman at}\\ \text{the bottom}}} \Big) \tag{6.20}$$

This is the governing equation for the ocean interior, away from the Ekman layers. It is driven by input of momentum at the surface and drag at the bottom.

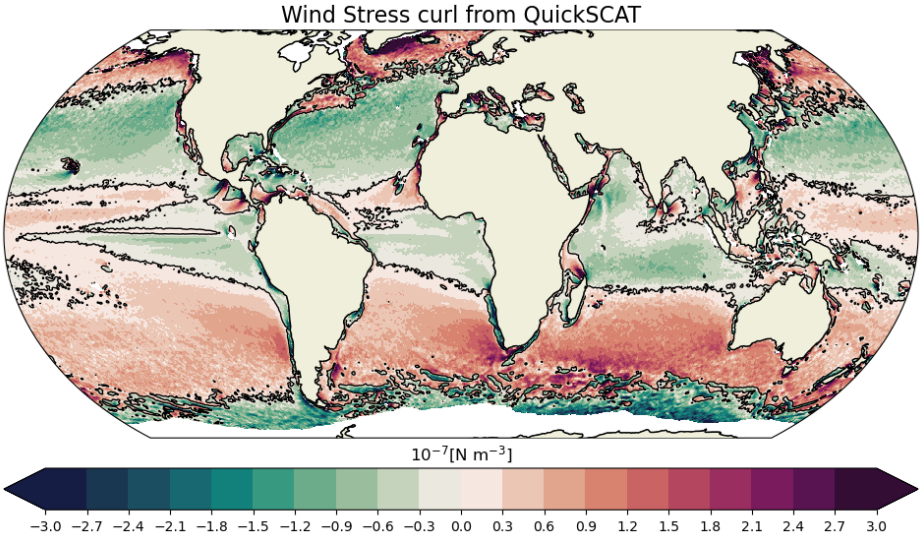

Figure 6.2: *Wind stress curl computed from QuickSCAT reanalysis [https://doi.org/10.1175/2008JPO3881.1].*

6.2 The Stommel model

We will now use the planetary-geostrophic equations. Let's define $\phi = p/\rho_0$ and $b = -g\rho'/\rho_0$. For a Boussinesq fluid, the planetary geostrophic equations are

$$\mathbf{f} \times \mathbf{u} = -\nabla\phi + \frac{1}{\rho_0}\frac{\partial \boldsymbol{\tau}}{\partial z} \tag{6.21}$$

$$\frac{\partial \phi}{\partial z} = b \tag{6.22}$$

$$\nabla_3 \cdot \mathbf{v} = 0. \tag{6.23}$$

The first equation is the horizontal momentum equation using geostrophic balance and a stress term. The second equation is the vertical momentum equation (hydrostatic balance). And the third is mass continuity.

The planetary geostrophic equations are essentially the Boussinesq primitive equations with the advection terms omitted in the horizontal momentum equation. They have been derived with a 'low Rossby number scaling', but for large scales, much larger than the deformation scale. Hence, this set of equations are composed of the geostrophic balance and the full mass continuity equations. These equations are not too useful in the atmosphere, where the deformation radius for a continuously stratified fluid, $L_d = \frac{NH}{f}$ (or $\frac{\sqrt{gH}}{f}$), is about 1000 km. Only the description of planetary waves can satisfy the PG equations. For the ocean, instead, where $L_d \simeq 100$ km, the PG equations are very useful, and used for the theory of large-scale circulation.

We now take the curl (or cross-differentiate) of (6.21) and find

$$\mathbf{f}\,\nabla \cdot \mathbf{u} + \frac{\partial f}{\partial y} v = curl_z \widetilde{\boldsymbol{\tau}} \tag{6.24}$$

where again $curl_z \boldsymbol{A} = \boldsymbol{k} \cdot \nabla \times \boldsymbol{A} = \partial_x A^y - \partial_y A^x$, and $\widetilde{\boldsymbol{\tau}} = \boldsymbol{\tau}/\rho_0$.

Now integrate over the full depth of the ocean

$$\int \mathbf{f}\,\nabla \cdot \mathbf{u}\,\mathrm{d}z + \frac{\partial f}{\partial y}\int v\,\mathrm{d}z = curl_z(\widetilde{\boldsymbol{\tau}}_T - \widetilde{\boldsymbol{\tau}}_B). \tag{6.25}$$

The first term vanishes, the divergence term, if the vertical velocities are zero at the top and bottom of the ocean. This is true for a flat-bottomed ocean but is not the case when topography will be added. We are thus left with:

$$\boxed{\beta \overline{v} = curl_z(\widetilde{\boldsymbol{\tau}}_T - \widetilde{\boldsymbol{\tau}}_B)}. \tag{6.26}$$

Where $\overline{A} = \int A \, \mathrm{d}z$. Eq. (6.26) is equivalent to Eq. (6.13), i.e. the SVERDRUP BALANCE, *a balance between the input of vorticity from the wind-stress curl and the advection of planetary vorticity*.

We now work on the rhs of (6.26). At the top the stress is given by the wind. At the bottom, which is flat for now, we parameterize the stress with a LINEAR DRAG, or Rayleigh friction, as it would be generated by an Ekman layer, and obtain

$$\boxed{\beta \overline{v} = F_\tau(x,y) - r\overline{\zeta}}. \tag{6.27}$$

Here the meridional flow is governed by

1. $F_\tau(x,y) = curl_z \widetilde{\boldsymbol{\tau}}_T$; the curl of the wind stress at the top of the ocean.
2. $\overline{\zeta} = \frac{\partial \overline{v}}{\partial x} - \frac{\partial \overline{u}}{\partial y}$; the vorticity of the vertically integrated flow
3. r; a linear drag or Rayleigh friction.

The flow velocity is divergent-free and we can define a streamfunction

$$\overline{u} = -\frac{\partial \psi}{\partial y} \quad \overline{v} = \frac{\partial \psi}{\partial x}$$

such that

$$\boxed{\beta \frac{\partial \psi}{\partial x} = F_\tau(x,y) - r\nabla^2 \psi}. \tag{6.28}$$

This is the **STOMMEL PROBLEM or MODEL**. The contribution of Stommel is the addition of a linear bottom drag that would balance the momentum input at the surface.

6.2.1 A homogeneous model

Instead of vertically integrating our momentum equations, we can instead consider a homogeneous layer of fluid, obeying the shallow water equations. The potential vorticity equation becomes

$$\frac{\mathrm{D}}{\mathrm{D}t}\Big(\frac{f+\zeta}{H}\Big) = \frac{F}{H}, \tag{6.29}$$

where F represents both forcing and friction. If the ocean is flat-bottomed and has a rigid lid, then

$$\frac{\mathrm{D}\zeta}{\mathrm{D}t} + \beta v = F. \tag{6.30}$$

This is the barotropic PV equation. Because of the rigid lid and flat-bottom, the flow is divergent-free, and we can express it with the usual streamfunction:

$$\boxed{\frac{\mathrm{D}}{\mathrm{D}\,t}\nabla^2\psi + \beta\frac{\partial\psi}{\partial x} = F_\tau(x,y) - r\nabla^2\psi}. \tag{6.31}$$

The first term of the l.h.s characterizes the *time-dependent, non-linear* STOMMEL MODEL. The steady non-linear model is simply

$$J(\psi,\nabla^2\psi) + \beta\frac{\partial\psi}{\partial x} = F_\tau(x,y) - r\nabla^2\psi. \tag{6.32}$$

Where the Jacobian is

$$J(A,B) = \frac{\partial A}{\partial x}\frac{\partial B}{\partial y} - \frac{\partial A}{\partial y}\frac{\partial B}{\partial x}. \tag{6.33}$$

And so the advective term is

$$u\frac{\partial\nabla^2\psi}{\partial x} + v\frac{\partial\nabla^2\psi}{\partial y} = \tag{6.34}$$

$$-\frac{\partial\psi}{\partial y}\frac{\partial\nabla^2\psi}{\partial x} + \frac{\partial\psi}{\partial x}\frac{\partial\nabla^2\psi}{\partial y} = \tag{6.35}$$

$$\frac{\partial\psi}{\partial x}\frac{\partial\nabla^2\psi}{\partial y} - \frac{\partial\psi}{\partial y}\frac{\partial\nabla^2\psi}{\partial x} = \tag{6.36}$$

$$J(\psi,\nabla^2\psi). \tag{6.37}$$

To recover the original Stommel model we need to ignore the advective derivative (the source of our non-linearities).

Take the barotropic PV equation (6.30) and perform a scale analysis of all terms:

$$\underbrace{\frac{\mathrm{D}\,\zeta}{\mathrm{D}\,t}}_{\frac{U}{L}\frac{U}{L}} + \underbrace{\beta v}_{\beta U} = F. \tag{6.38}$$

Let's define $Z = \frac{U}{L}$ a representative value for vorticity, so that in order to ignore nonlinearities the following inequality must hold: $Z \ll \beta L$, or

$$R_\beta = \frac{U}{\beta L^2} \ll 1 \tag{6.39}$$

which is called the β Rossby number[1]. Assuming a β Rossby number much smaller than unity is equivalent to the small Rossby number assumption used to obtain the PG equations.

[1]Remember that the Rossby number is $R_o = \frac{U}{fL}$

The response to an input of vorticity: relative vorticity or planetary vorticity?

Recalling the PV equation

$$\frac{\mathrm{D}}{\mathrm{D}t}\Big(\frac{f+\zeta}{H}\Big) = \frac{F}{H}, \tag{6.40}$$

The ocean will respond to an input of vorticity F by either changing ζ or f. Using the above scaling approach we see that

$$\underbrace{\frac{\mathrm{D}\zeta}{\mathrm{D}t}}_{\frac{U^2}{L^2}} + \underbrace{\beta v}_{\beta U} = F. \tag{6.41}$$

The ratio of relative vorticity and advection of planetary vorticity is

$$\frac{\mathrm{D}\zeta}{\mathrm{D}t} \Big/ \frac{\mathrm{D}f}{\mathrm{D}t} \sim \frac{U}{\beta L^2} \equiv R_\beta. \tag{6.42}$$

- Consider now the basin scale (L ∼1000 km, U ∼0.01 m s^{-1}). The β Rossby number would be

$$R_\beta = \frac{U}{\beta L^2} = \frac{10^{-2}}{10^{-11}(10^6)^2} = 10^{-3}. \tag{6.43}$$

  Within the basin scale, the rate of change of relative vorticity is small compared to the rate of change of planetary vorticity. This means that an input of vorticity, say from the wind, does not induce the flow to increase its rotation, rather it will force the flow to move meridionally to reach a balance through f.

- Now consider a frontal zone instead (L ∼10 km, U ∼0.1 m s^{-1}). The β Rossby number would be

$$R_\beta = \frac{U}{\beta L^2} = \frac{10^{-1}}{10^{-11}(10^4)^2} = 10^{2}. \tag{6.44}$$

  Within a frontal zone, the rate of change of ζ is much larger than β. This means that the ocean will respond to F by changing ζ.

The response is thus fundamentally different, and the two regions will be governed by different dynamics: there will be a large *interior* regime and a narrow *boundary layer* regime.

6.2.2 The interior: Sverdrup balance

The Stommel model is linear, and we can obtain analytical solutions

$$\boxed{\beta \frac{\partial \psi}{\partial x} = F_\tau(x,y) - r\nabla^2\psi} \tag{6.45}$$

First, note that the Stommel model was previously derived by the β-plane approximation to the primitive equations:

$$\beta \frac{\partial p}{\partial x} = \frac{f_0}{H} curl_z \boldsymbol{\tau} - \frac{f_0 d}{2H}\nabla^2 p. \tag{6.46}$$

Now, let's have a look at the relative role of the top and bottom Ekman contributions. The ratio between the pressure gradient term and the frictional term is

$$\frac{f_0 d}{2H} P/L^2/(\beta P/L) \rightarrow \frac{f_0 d}{2H\beta L} \tag{6.47}$$

Typical values can be used for d $\sim$15 m, f_0 $\sim 10^{-4}$, β $\sim 10^{-11}$, H $\sim$3000 m and L $\sim$1000 km, and the ratio is $\sim$0.02. This implies that the frictional term can be neglected and that the Ekman pumping induced by the wind stress is much larger than the one resulting from bottom friction.

This approximation will lead us towards our first solution

$$\beta \frac{\partial p}{\partial x} = \frac{f_0}{H} curl_z \tau, \tag{6.48}$$

which implies a meridional velocity that is a function of the wind-stress curl, and is best known as *Sverdrup balance*.

Suppose, in fact, that the frictional term is small, so there is an approximate balance between the input of vorticity by the wind stress and the β-effect (or the rate of change of planetary vorticity).

Friction is small if

$$|r\zeta| \ll |\beta v|. \tag{6.49}$$

If we define $r = \frac{f_0 \delta}{H}$, as suggested by (6.46), where δ is the thickness of the bottom Ekman layer, then

$$\frac{f_0 \delta}{H}\frac{U}{L} \ll \beta U, \quad \text{or} \quad \frac{r}{L} \ll \beta. \tag{6.50}$$

This inequality is well satisfied in large-scale flows, where L is the horizontal scale of the motion. The vorticity equations is thus

$$\beta \frac{\partial \psi}{\partial x} = F_\tau(x,y) \tag{6.51}$$

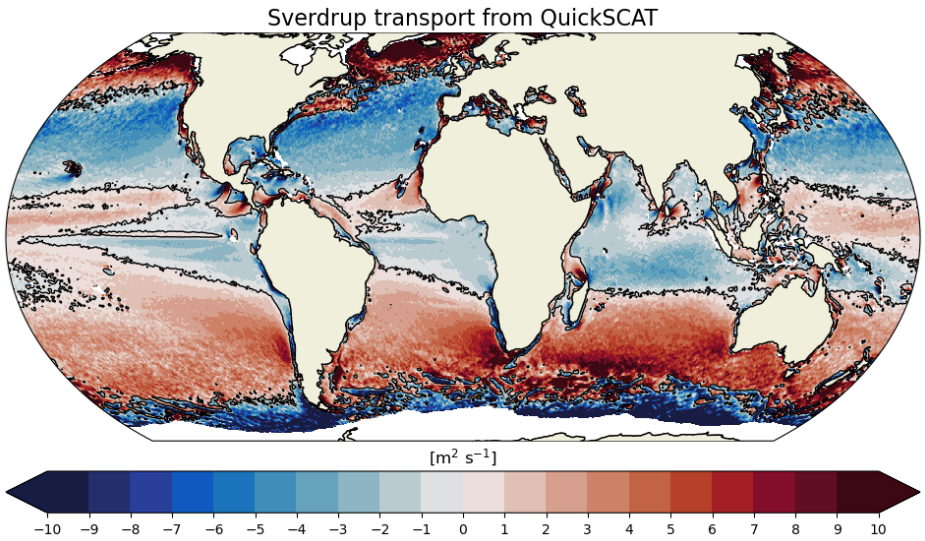

Figure 6.3: *Estimate of Sverdrup transport computed from QuickSCAT as* $\overline{v} = curl_z\widetilde{\boldsymbol{\tau}}/\beta$.

which is just an expression of Sverdrup balance

$$\boxed{\beta\overline{v} = curl_z\widetilde{\boldsymbol{\tau}}} \tag{6.52}$$

This is equivalent to the linear geostrophic vorticity balance

$$\beta v = f_0\frac{\partial w}{\partial z} \tag{6.53}$$

where stress at the bottom is neglected. In fact, over most of the ocean, the deep flow is very weak, meaning that bottom drag is negligible.

Eq.6.52 is not a transport, rather just a balance between wind stress at the surface and the β-effect leading to a meridional velocity $\overline{v} = \frac{1}{\beta}curl_z\tau$ (Fig. 6.3).

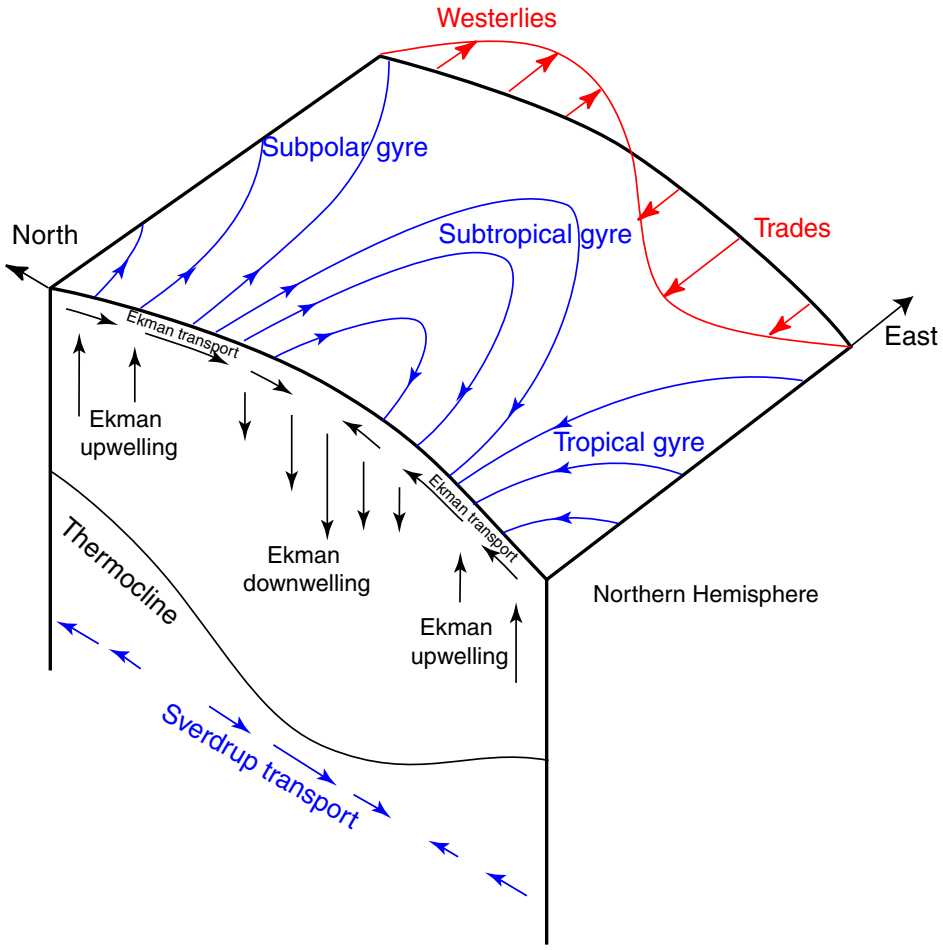

Figure 6.4: *Sverdrup balance circulation ($f > 0$). [from Talley et al. (2011)]*

Physical interpretation

Consider a schematic of the subtropical North Pacific. The winds at the sea surface are not spatially uniform. South of about 30°N, the Pacific is dominated by easterly trade winds. North of this, it is dominated by the westerlies. This causes northward Ekman transport under the trade winds, and southward Ekman transport under the westerlies. As a result, there is Ekman convergence throughout the subtropical North Pacific.

The convergent surface layer water in the subtropics must go somewhere so there is downward vertical velocity at the base of the (50 m thick) Ekman layer. At some level between the surface and ocean bottom, there is likely no vertical velocity. Therefore there is net "squashing" of the water columns in the subtropical region (*Ekman pumping*).

This squashing requires a decrease in either planetary or relative vor-

ticity (remember potential vorticity conservation $\frac{D}{Dt}\frac{f+\zeta}{H} = 0$). In the ocean interior, relative vorticity is small, so planetary vorticity must decrease, which results in the equatorward flow that characterizes the subtropical gyre (Fig. 6.4).

The subpolar North Pacific lies north of the westerly wind maximum at about 40°N. Ekman transport is therefore southward, with a maximum at about 40°N and weaker at higher latitudes. Therefore there must be upwelling (*Ekman suction*) throughout the wide latitude band of the subpolar gyre. This upwelling stretches the water columns, which then move poleward, creating the poleward flow of the subpolar gyre.

The Sverdrup transport is the net meridional transport diagnosed in both the subtropical and subpolar gyres, resulting from *planetary vorticity changes that balance Ekman pumping or Ekman suction*. All of the meridional flow is returned in western boundary currents, for reasons described in the following sections. Therefore, subtropical gyres must be anticyclonic and subpolar gyres must be cyclonic.

Computing the transport

Assuming the ocean circulation is in Sverdrup balance, $\overline{v} = \frac{\partial \psi}{\partial x}$ gives the meridional mass transport of the vertically integrated column of fluid due to a surface wind stress. The constraint that there be no normal flow across the ocean's horizontal boundaries means that $\psi = const$ on the boundaries. We pick this constant arbitrarily to be 0. We must choose whether to choose the eastern or western boundary as the limit of integration. This cannot be determined by Sverdrup balance alone, it requires consideration of frictional boundary layers.

We choose the eastern boundary, requiring closure of the circulation in a western boundary current, and we require that the streamfunction be zero on the eastern boundary.

Integrating from east to west, and using the boundary condition $\psi = 0$ at $x = x_E(y)$, the streamfunction is (see Fig. 6.5 and Fig. 6.6)

$$\begin{aligned} \int_x^{x_E} \frac{\partial \psi}{\partial x}\,\mathrm{d}x' &= \frac{1}{\beta}\int_x^{x_E} curl_z \widetilde{\boldsymbol{\tau}}_T\,\mathrm{d}x \\ \psi(x,y) &= -\frac{1}{\beta}\int_x^{x_E} curl_z \widetilde{\boldsymbol{\tau}}_T\,\mathrm{d}x. \end{aligned}$$

Two examples are shown in Fig. 6.5 for the North Atlantic and the North Pacific. The Sverdrup balance gives a reasonable good estimation

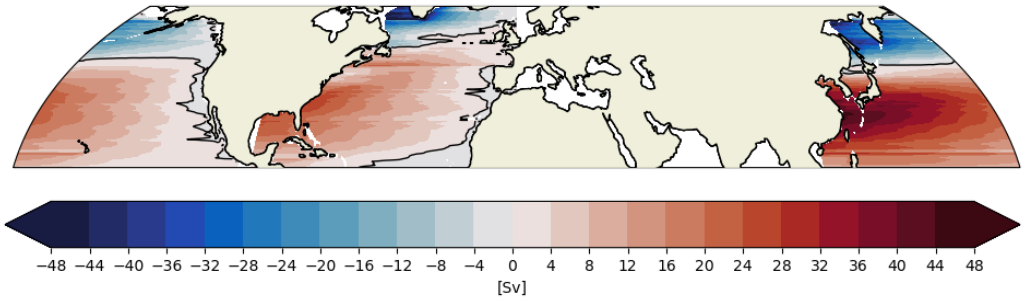

Figure 6.5: *Estimate of the depth-integrated circulation (in Sv) predicted by the Sverdrup balance in the North Atlantic and the North Pacific computed with QuickSCAT winds. The solution assumes that the depth-integrated circulation vanishes at the eastern boundary. Positive values (red) correspond to clockwise circulations and negative values (blue) to anticlockwise circulations.*

for the interior flow, but a western boundary current is needed to close the circulation. The Sverdrup balance integration results in a realistic large-scale gyre circulation in the tropical, subtropical and subpolar oceans (Fig. 6.6). However something is not well represented and totally missed by the Sverdrup flow. Sverdrup flow predicts an interior flow in balance with the input of vorticity by the wind stress; but the interior meridional flow must be compensated at some level somewhere to comply with mass conservation. This, we will see, is accomplished by a narrow and intense boundary current.

In the Southern Ocean, the zonal integration of the Sverdrup balance does not apply. We will see in Chapter **??** what is so special about the Southern Ocean.

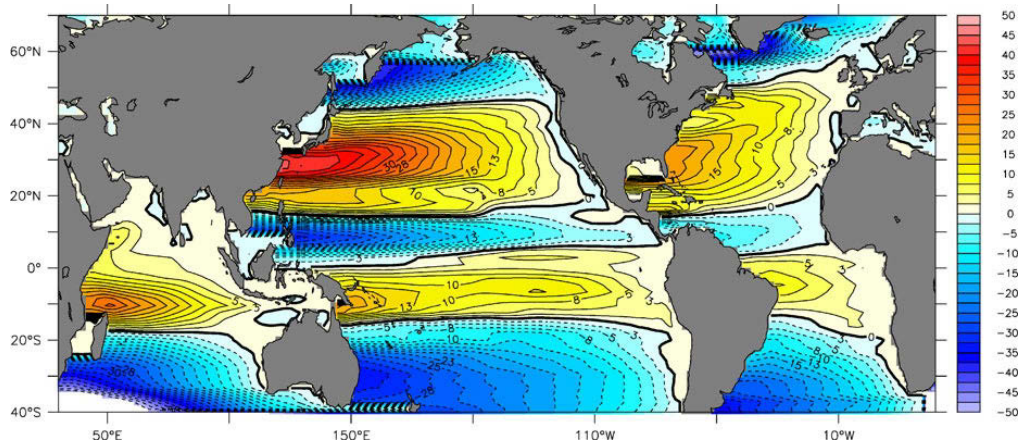

Figure 6.6: *Streamfunction ψ ($Sv \equiv 10^6\ m^3\ s^{-1}$) calculated from the Sverdrup relation and a climatological wind stress curl. Westward integration starts at 30° E with $\psi = 0$ as boundary condition. [from Olbers et al. (2012)]*

6.2.3 The boundary: Adding a return flow

We need to close the circulation induced by the interior Sverdrup flow. The interior flow was developed for the large scale. We can thus suppose that the return flow will occur in a narrow boundary layer somewhere. Where will this be? Western or eastern side of the basin?

Take the full Stommel model

$$\beta \frac{\partial \psi}{\partial x} = curl_z \boldsymbol{\tau}_T - r\nabla^2 \psi. \tag{6.54}$$

and consider a square domain of side L and rescale variables as follows

$$\begin{aligned} x = L\,\hat{x} \quad \tau = \tau_0\,\hat{\tau} \\ y = L\,\hat{y} \quad \psi = \frac{\tau_0}{\beta}\,\hat{\psi} \end{aligned}$$

Hatted variables are non-dimensional and they are $\mathcal{O}(1)$ quantities in the interior.

The Stommel model becomes

$$\begin{aligned} \beta \frac{\partial \hat{\psi}}{\partial \hat{x}} \frac{\tau_0}{\beta L} &= curl_z \hat{\boldsymbol{\tau}}_T \frac{\tau_0}{L} - r\nabla^2 \hat{\psi} \frac{\tau_0}{\beta L^2} \\ \frac{\partial \hat{\psi}}{\partial \hat{x}} &= curl_z \hat{\boldsymbol{\tau}}_T - \frac{r}{\beta L} \nabla^2 \hat{\psi} \end{aligned}$$

$\epsilon_s = \frac{r}{\beta L} \ll 1$ as shown by (6.50) for the large-scale flow. We thus write a solution for the interior, where friction is small, and a solution for the boundary, where frictional effects will be large:

$$\psi(x,y) = \psi_I(x,y) + \phi(x,y)$$

where ϕ is a boundary layer correction.

The interior solution

In the interior the flow is described by $\psi_I(x,y)$ in the limit where $\epsilon_s = \frac{r}{\beta L} \ll 1$

$$\frac{\partial \psi_I}{\partial x} = curl_z \boldsymbol{\tau}_T \tag{6.55}$$

The solution of the Sverdrup interior is

$$\psi_I(x,y) = \int_0^x curl_z \boldsymbol{\tau}(x',y) \mathrm{d}x' + g(y) \tag{6.56}$$

where $g(y)$ is an arbitrary function. Given the streamfunction definition ($v_I = \partial\psi_I/\partial x$; $u_I = -\partial\psi_I/\partial y$), the corresponding velocities are

$$\begin{aligned} v_I &= curl_z\boldsymbol{\tau} \\ u_I &= -\partial_y \int_0^x curl_z\boldsymbol{\tau}(x',y)\,\mathrm{d}x' - \frac{\partial g(y)}{\partial y} \end{aligned}$$

Let's simplify our forcing and take the wind stress curl as zonally uniform, so that

$$\tau_T^y = 0, \quad \tau_T^x = -cos(\pi y) \tag{6.57}$$

so that the curl vanishes at $y = 0$ and $y = 1$ (Fig. 6.7). The curl in this case will be $curl_z\boldsymbol{\tau}_T = -\pi sin(\pi y)$. For this example, typical of subtropical latitudes, the wind stress is imparting a negative input of vorticity into the ocean everywhere.

The Sverdrup interior flow is

$$\begin{aligned} \psi_I(x,y) &= \int_0^x curl_z\boldsymbol{\tau}(x',y)\mathrm{d}x' + g(y) \\ \psi_I(x,y) &= \int_0^x \Big[-\pi sin(\pi y)\Big]\,\mathrm{d}x' + g(y) \\ \psi_I(x,y) &= x\Big[-\pi sin(\pi y)\Big] + g(y) \end{aligned}$$

We can define the arbitrary function of integration as $C(y) = -g(y)/curl_z\boldsymbol{\tau}_T$. So that our solution becomes

$$\begin{aligned} \psi_I(x,y) &= x\Big[-\pi sin(\pi y)\Big] - \Big[C(y) curl_z\boldsymbol{\tau}_T\Big] \\ \psi_I(x,y) &= x\Big[-\pi sin(\pi y)\Big] + C(y)\Big[\pi sin(\pi y)\Big] \\ \psi_I(x,y) &= \pi\Big[C(y) - x\Big] sin(\pi y) \end{aligned}$$

If C is a constant, then the zonal flow is $C\,curl_z\boldsymbol{\tau}$. Now, depending on C, we can either satisfy $\psi = 0$ at $x = 0$ or at $x = 1$

$$\psi_I(0,y) = \pi C\,sin(\pi y) = 0 \qquad \text{if} \quad C = 0 \tag{6.58}$$

$$\psi_I(1,y) = \pi(C-1)\,sin(\pi y) = 0 \quad \text{if} \quad C = 1 \tag{6.59}$$

We cannot satisfy both zonal boundary conditions of $\psi = 0$. And so a choice will have to be made on C, and more importantly on where the

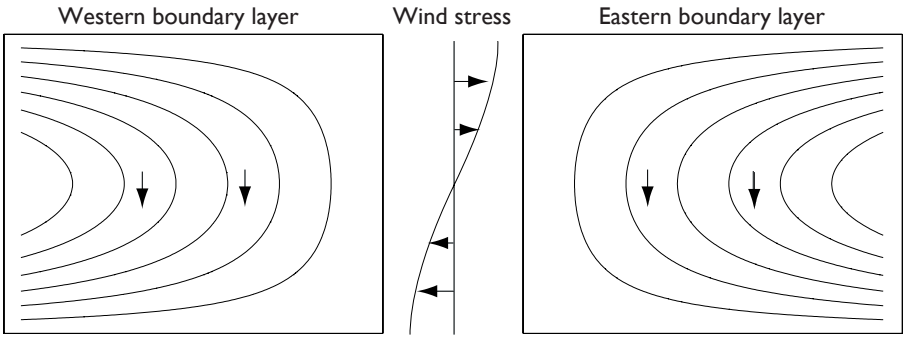

Figure 6.7: *Two possible Sverdrup flows, ψ_I, for the given wind stress. Each solution satisfies the no-flow condition at one boundary, either east or west. Both solutions have the same meridional interior flow. Which one is physically plausible? [from Vallis (2006)]*

boundary layer will exist in order to satisfy the remaining boundary condition!

We could suppose the solution at the left of Fig.6.7, because the interior flow would go the same direction as the wind torque driving it. Friction should provide opposite torque in order to balance the angular momentum. An eastern boundary (solution at the right of Fig.6.7) would not be able to provide an anti-clockwise angular momentum (vorticity) capable of balancing vorticity input by the surface stress. Only the Western Boundary Current seems able to provide the required frictional force. We will expand on this 'vorticity argument' in Section 6.4

The boundary solution (asymptotic matching)

Let's now stretch the x-coordinate near the boundary, where $\phi(x, y)$ varies very rapidly in order to satisfy the boundary condition. The boundary could be at $x = 0$ or at $x = 1$:

$$x = \epsilon\,\alpha \quad \text{or} \quad x - 1 = \epsilon\,\alpha. \tag{6.60}$$

α is the stretched coordinate, having values $\mathcal{O}(1)$ in the boundary and ϵ is a small parameter. We now suppose $\phi(\alpha, y)$ and write:

$$\partial_x(\psi_I + \phi) + \epsilon_s\nabla^2(\psi_I + \phi) = curl_z\boldsymbol{\tau}_T \tag{6.61}$$

$$\partial_x\psi_I + \epsilon_s(\nabla^2\psi_I + \nabla^2\phi) + \frac{1}{\epsilon}\frac{\partial\phi}{\partial\alpha} = curl_z\boldsymbol{\tau}_T \tag{6.62}$$

$$\tag{6.63}$$

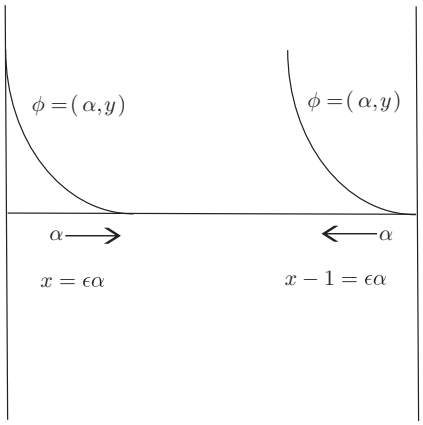

Figure 6.8: *Two possible boundary solutions. Only the one on the western side decays towards the interior and satisfies the condition that $\phi = 0$ in the interior. The solution requires that $\alpha > 0$ and $x = \epsilon\alpha$.*

where $\nabla^2\phi = \frac{1}{\epsilon^2}\frac{\partial^2\phi}{\partial\alpha^2} + \frac{\partial^2\phi}{\partial y^2}$. We know that ϕ_I satisfies Sverdrup balance, so the solution becomes

$$\epsilon_s(\nabla^2\psi_I + \frac{1}{\epsilon^2}\frac{\partial^2\phi}{\partial\alpha^2} + \frac{\partial^2\phi}{\partial y^2}) + \frac{1}{\epsilon}\frac{\partial\phi}{\partial\alpha} = 0. \tag{6.64}$$

We now make the simplest choice and choose $\epsilon = \epsilon_s$, so that the leading order balance is

$$\frac{\partial^2\phi}{\partial\alpha^2} + \frac{\partial\phi}{\partial\alpha} = 0. \tag{6.65}$$

The solution of which is $\phi = A(y) + B(y)e^{-\alpha}$.

The solution grows in the negative direction of α. But the solution cannot grow towards the interior or it would violate our assumption that ϕ is small in the interior. Hence, we impose $\alpha > 0$ and $A(y) = 0$. This implies the choice of $x = \epsilon\alpha$ so that $\alpha > 0$ for $x > 0$. The boundary layer is at $x = 0$: *a western boundary layer*, and it decays eastward for increasing α, towards the interior (Fig. 6.8).

We now choose $C = 1$, so that $\psi_I = 0$ at $x = 1$, and the solution for the given wind stress is

$$\psi_I = \pi(1 - x)\, sin(\pi y) \tag{6.66}$$

This satisfies the eastern boundary condition ($\psi = 0$ at $x = 1$).

$B(y)$ will now satisfy the other boundary condition in order to

$$\psi = \psi_I + \phi = 0 \quad \text{at} \quad x = 0. \tag{6.67}$$

At $x = 0$:

$$\psi = \pi \sin(\pi y) + \phi = 0 \tag{6.68}$$

Given that $\phi = B(y)e^{-\alpha}$, we have, at $x = 0$

$$\psi = \pi \sin(\pi y) + B(y) = 0, \tag{6.69}$$

which readily implies that $B(y) = -\pi \sin(\pi y)$. The boundary layer correction is thus

$$\phi = -\pi \sin(\pi y) e^{-x/\epsilon_s}. \tag{6.70}$$

The boundary layer correction is thus proportional to the interior wind stress, as it has to balance that input of vorticity.

The full solution is thus

$$\begin{aligned} \psi = \psi_I + \phi &= \pi \sin(\pi y) - x\pi \sin(\pi y) - \pi \sin(\pi y) e^{-x/\epsilon_s} && (6.71) \\ &= \pi \sin(\pi y)\Big(1 - x - e^{-x/\epsilon_s}\Big). && (6.72) \end{aligned}$$

The dimensional solution (remember that $\psi = \hat{\psi}\frac{\tau_0}{\beta}; \tau = \hat{\tau}\tau_0; y = \hat{y}L; x = \hat{x}L$):

$$\boxed{\psi = \frac{\tau_0}{\beta}\pi\Big(1 - \frac{x}{L} - e^{-x/(L\epsilon_s)}\Big) \sin\frac{\pi y}{L}} \tag{6.73}$$

Given the chosen wind stress, this is a single gyre solution (Fig. 6.9), and for a realistic global wind stress the solution is shown in Fig. 6.11.

The boundary layer width

What is the width δ of the western boundary layer? In the interior, friction is small, and the balance is between wind stress and the β-effect:

$$|r\zeta| \ll |\beta v|. \tag{6.74}$$

With $r = \frac{f\delta}{H}$, this means that $\frac{f\delta}{HL} \ll \beta$. For friction to be small, we also have that

$$\epsilon_s = \frac{r}{L\beta} \ll 1 \quad \text{or} \quad \frac{r}{\beta} \ll L, \tag{6.75}$$

where r measures bottom friction and L denotes the length scale of zonal variations of the geostrophic current.

However, when L becomes smaller, representing dynamics in the boundary layer, we have a different balance:

$$\frac{r}{\beta} \sim L, \tag{6.76}$$

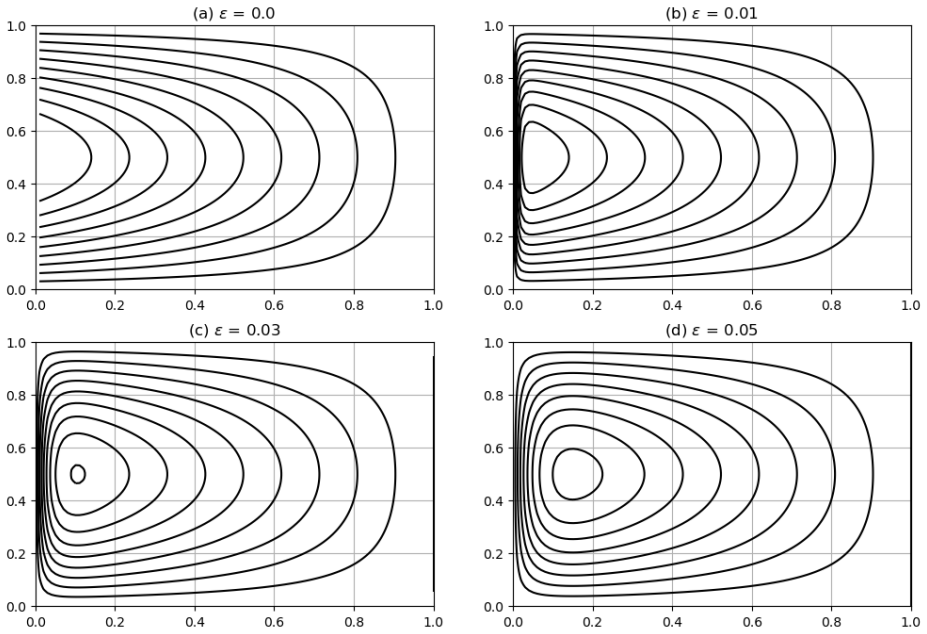

Figure 6.9: *Solutions of the Stommel model for a single-gyre wind-induced flow for different values of ϵ. Note that for ϵ=0 the model reduces to the Sverdrup balance.*

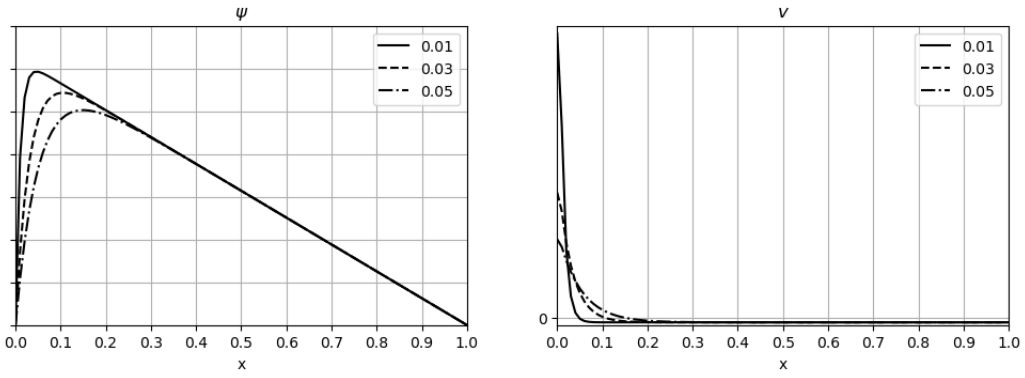

Figure 6.10: *Solutions of the Stommel model for a single-gyre wind-induced flow for different values of ϵ. Plotted are the streamfunction ψ and the meridional velocity $v = \partial\psi/\partial x$ at the centre of the gyre.*

and now $L = \mathcal{O}(\delta)$ so that the width of the Stommel boundary layer is

$$\boxed{\delta_S = \frac{r}{\beta}}. \tag{6.77}$$

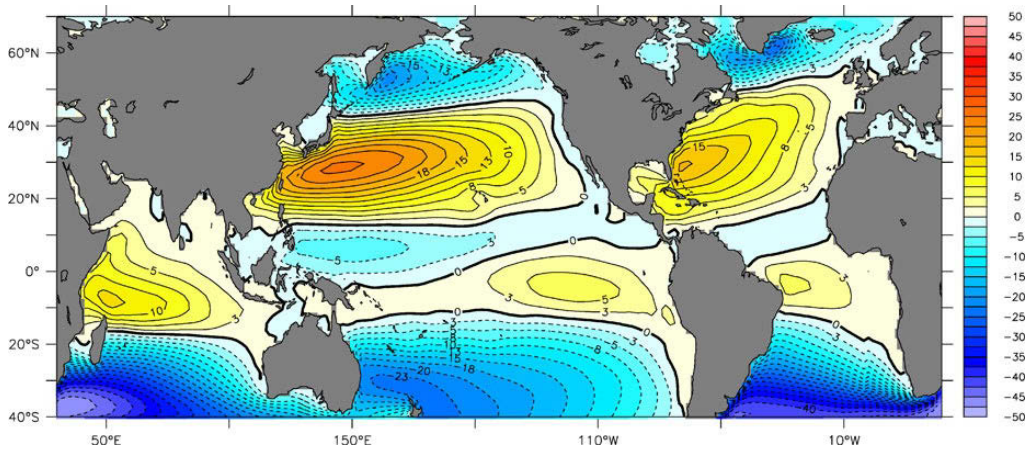

Figure 6.11: *Streamfunction ψ (in Sv) computed from the Stommel model with realistic wind stress curl and a boundary layer width δ = 100 km. [from Olbers et al. (2012)]*

Within this narrow boundary layer, $v_g > 0$ and $\overline{v} > 0$, balancing the interior Sverdrup flow. The total transport in the Sverdrup regime occurs between the eastern edge of the western boundary layer, $x = \delta_S$, and the eastern coast, $x = 1$. A corresponding transport must be compensated and returned within the boundary layer. This transport is thus prescribed by the wind outside the boundary layer, the Sverdrup regime. Because the boundary layer width is much smaller than the basin width, the currents in the boundary layer have to be much stronger than in the Sverdrup regime, as observed.

An f-plane solution

In the Stommel model, dissipation of vorticity arises from bottom frictional stresses within a bottom boundary layer.

In the case of a constant f, so that $\beta = \frac{\partial f}{\partial y} = 0$, the input of vorticity from the wind simply balances the opposing frictional dissipation everywhere. This leads to symmetric solutions, which are not realistic.

$$\underbrace{\beta \frac{\partial \psi}{\partial x}}_{\substack{0 \text{ for} \\ \text{the } f\text{-plane}}} = \underbrace{F_\tau(x,y)}_{\substack{\text{wind input} \\ \text{of vorticity}}} \qquad \underbrace{-r\nabla^2\psi}_{\substack{\text{frictional dissipation} \\ \text{of vorticity}}} \quad . \tag{6.78}$$

The vertical geostrophic velocity vanishes in the f-plane, and the two Ekman induced vertical velocities have to compensate each other. This is possible if

$$curl_z \widetilde{\boldsymbol{\tau}}_T = curl_z \widetilde{\boldsymbol{\tau}}_B = \frac{d}{2}\zeta_g \tag{6.79}$$

There is no boundary layer solution, and the balance is achieved everywhere within the basin (see Fig. 6.12).

If, conversely, $\beta \neq 0$, in the interior we find a balance between change in planetary vorticity and input of vorticity. In the narrow western boundary layer, the fluid column changes again its planetary vorticity but the source of vorticity is from frictional dissipation.

But given that the return flow was found on a western boundary layer, is bottom drag realistic?

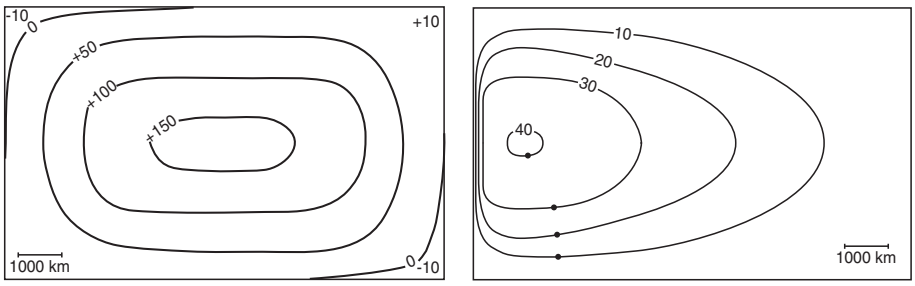

Figure 6.12: *Stommel's wind-driven circulation solution for a subtropical gyre with trades and westerlies. (a) Transport streamfunction ψ on a uniformly rotating Earth ($f = f_0$) and (b) westward intensification with the β-effect ($f = f_0 + \beta y$). [from Stommel (1948)]*

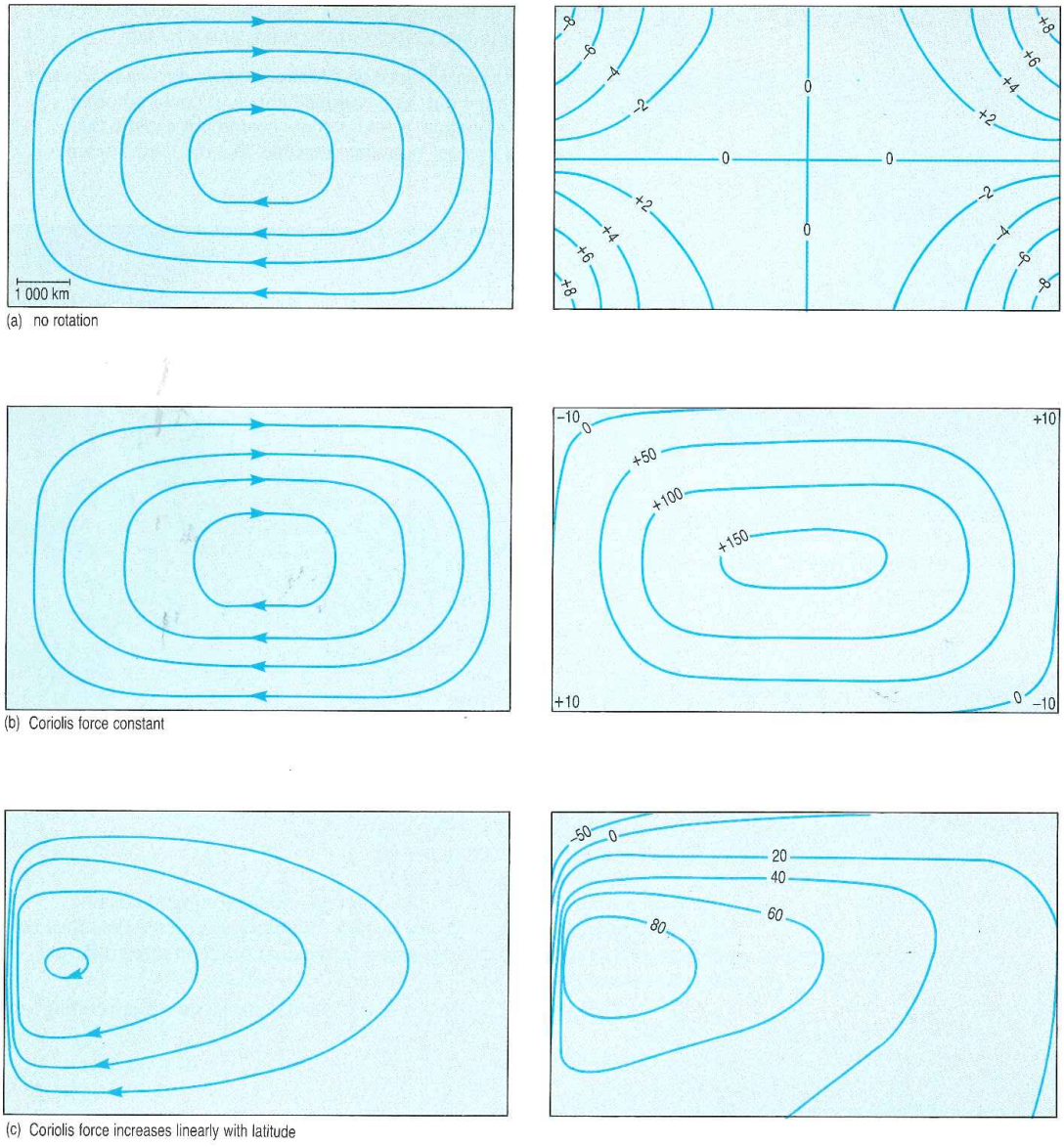

Figure 6.13: *(left panels) Streamfunction ψ and (right panels) sea-surface height η for a symmetrical gyral wind field (à la Stommel). In the case of no rotation $f = 0$ winds simply drive a symmetric circulation, just as you might expect from stirring a coffee cup. If f =const and $\beta = 0$ as in a flat Earth, there is again a symmetric solution with fluid rotating in geostrophic balance. Western intensification requires Earth to be a spinning sphere with planetary vorticity varying with latitude. [from Stommel (1948)]*

6.3 The Munk model

An Ekman bottom drag is not appropriate to balance the interior wind-driven circulation. This is because the circulation does not reach all the way down to the bottom and some other form/term is required to balance the interior transport. An extension of the Stommel problem was formulated by Munk, who introduced lateral harmonic viscosity.

Munk does not use a bottom drag and, given that the boundary layer is on a side, introduces horizontal viscosity. We can start from the set of primitive equations and our fluid is governed by

$$-fv = -\frac{\partial \phi}{\partial x} + \frac{\partial}{\partial x}\left(\frac{\nu_h}{\rho_0}\frac{\partial u}{\partial x}\right) + \frac{\partial}{\partial y}\left(\frac{\nu_h}{\rho_0}\frac{\partial u}{\partial y}\right) + \frac{\partial}{\partial z}\left(\frac{\nu_v}{\rho_0}\frac{\partial u}{\partial z}\right) \quad (6.80)$$

$$fu = -\frac{\partial \phi}{\partial y} + \frac{\partial}{\partial x}\left(\frac{\nu_h}{\rho_0}\frac{\partial v}{\partial x}\right) + \frac{\partial}{\partial y}\left(\frac{\nu_h}{\rho_0}\frac{\partial v}{\partial y}\right) + \frac{\partial}{\partial z}\left(\frac{\nu_v}{\rho_0}\frac{\partial v}{\partial z}\right) \quad (6.81)$$

$$0 = \frac{\partial u}{\partial x} + \frac{\partial v}{\partial y} + \frac{\partial w}{\partial z} \quad (6.82)$$

or in a simpler form

$$\mathbf{f} \times \boldsymbol{u} = -\nabla \phi + \frac{1}{\rho_0} \nabla \cdot (\nu \nabla \boldsymbol{u}) \quad (6.83)$$

$$\nabla_3 \cdot \boldsymbol{u} = 0 \quad (6.84)$$

which are very similar to the set of equations used by Stommel (Eq. 6.21), but now we have introduced a term related to horizontal turbulent viscosity. These will be the key to introduce a frictional dissipation similar to the Stommel bottom drag.

Again, assume a vertically-integrated ocean, let's vertically integrate and pose:

$$\Phi = \int_{-H}^{z} \phi \, \mathrm{d}z; \quad \overline{u} = \int_{-H}^{z} \rho_0 u \, \mathrm{d}z; \quad \overline{v} = \int_{-H}^{z} \rho_0 v \, \mathrm{d}z \quad (6.85)$$

we find

$$-f\overline{v} = -\frac{\partial \Phi}{\partial x} + \nu_h \nabla^2 \overline{u} + \int_{-H}^{z} \frac{\partial}{\partial z} \nu_v \frac{\partial u}{\partial z} \, \mathrm{d}z \quad (6.86)$$

$$f\overline{u} = -\frac{\partial \Phi}{\partial y} + \nu_h \nabla^2 \overline{v} + \int_{-H}^{z} \frac{\partial}{\partial z} \nu_v \frac{\partial v}{\partial z} \, \mathrm{d}z \quad (6.87)$$

$$0 = \frac{\partial \overline{u}}{\partial x} + \frac{\partial \overline{v}}{\partial y} \quad (6.88)$$

We have set $w = 0$ at $z = 0$ and $z = -H$, and note that the stress tensor was defined as

$$\tau^x = \left(\nu_v \frac{\partial u}{\partial z}\right)_{z=0} - \left(\nu_v \frac{\partial u}{\partial z}\right)_{z=-H} \tag{6.89}$$

$$\tau^y = \left(\nu_v \frac{\partial v}{\partial z}\right)_{z=0} - \left(\nu_v \frac{\partial v}{\partial z}\right)_{z=-H}. \tag{6.90}$$

Ignoring bottom contributions this yields

$$-f\overline{v} = -\frac{\partial \Phi}{\partial x} + \nu_h \nabla^2 \overline{u} + \tau_T^x \tag{6.91}$$

$$f\overline{u} = -\frac{\partial \Phi}{\partial y} + \nu_h \nabla^2 \overline{v} + \tau_T^y \tag{6.92}$$

$$0 = \frac{\partial \overline{u}}{\partial x} + \frac{\partial \overline{v}}{\partial y}. \tag{6.93}$$

Now, as usual, take the curl of the horizontal momentum equations and use a streamfunction for the non-divergent flow to obtain:

$$\boxed{\beta \frac{\partial \psi}{\partial x} = curl_z \boldsymbol{\tau}_T + \nu_h \nabla^4 \psi} \tag{6.94}$$

The operator $\nu_h \nabla^4$ parameterizes viscosity as a biharmonic turbulent viscosity. This simple model captures a western boundary 'return' current and an interior Sverdrup flow. The simple model points to the role of the wind stress curl, and not the wind *per se*. The strength of the return current is dictated by dynamics outside of the boundary layer itself, i.e. the interior wind stress curl. This explains why some boundary currents (the Gulf Stream) are stronger than others (the Brazil current), which are driven by weaker wind stress curl (Fig. 6.14).

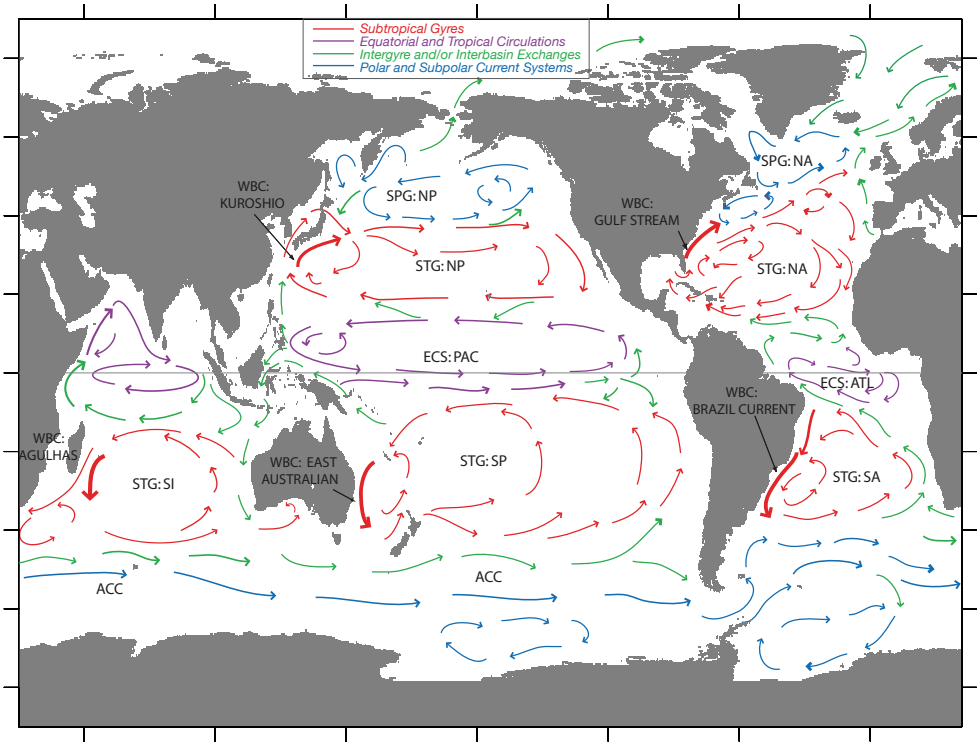

Figure 6.14: *A schema of the main currents of the global ocean [from Vallis (2006)].*

6.3.1 Interior and boundary solutions

The vorticity equation now reads

$$\boxed{\beta\frac{\partial\psi}{\partial x} = curl_z\boldsymbol{\tau}_T + \nu_h\nabla^2\zeta = curl_z\boldsymbol{\tau}_T + \nu_h\nabla^4\psi}. \tag{6.95}$$

This is the so-called MUNK MODEL. We need two boundary conditions at each wall because of the higher-order term. One is $\psi = 0$ to satisfy no-normal flow condition. The second boundary condition could be:

1. Zero vorticity ($\zeta = 0$). Since $\psi = 0$ along the boundary, this is equivalent to $\frac{\partial^2\psi}{\partial n^2} = 0$, where $\frac{\partial}{\partial_n}$ denotes a derivative normal to the boundary. At $x = 0$, this condition becomes $\frac{\partial v}{\partial x} = 0$: there is no horizontal shear at the boundary. This is called a '*free-slip*' condition.

2. No flow along the boundary. This is equivalent to $\frac{\partial\psi}{\partial n} = 0$. At $x = 0$, this condition becomes $v = 0$. This is called a '*no-slip*' condition.

Either could be used, and we will solve the '*no-slip*' problem. If we use the same wind stress

$$\tau^x = -cos(\pi y/L), \tag{6.96}$$

and non-dimensionalize (6.95) in a similar way to the Stommel problem

$$\frac{\partial\hat{\psi}}{\partial\hat{x}} - \epsilon_M\nabla^4\hat{\psi} = curl_z\widetilde{\boldsymbol{\tau}}_T. \tag{6.97}$$

Here $\epsilon_M = \nu/(\beta L^3)$. Again, the full solution will be the contribution of a western boundary layer correction and an interior Sverdrup flow

$$\hat{\psi} = \psi_I + \phi(\alpha, y). \tag{6.98}$$

The Munk problem does become

$$-\epsilon_M\Big(\nabla^4\psi_I + \frac{1}{\epsilon^4}\frac{\partial^4\phi}{\partial\alpha^4}\Big) + \frac{1}{\epsilon}\frac{\partial\phi}{\partial\alpha} = 0. \tag{6.99}$$

Of which the leading order balance is

$$-\frac{\partial^4\phi}{\partial\alpha^4} + \frac{\partial\phi}{\partial\alpha} = 0. \tag{6.100}$$

Subject to suitable boundary conditions and the interior Sverdrup solution

$$\psi_I = \pi(1-x)sin(\pi y), \tag{6.101}$$

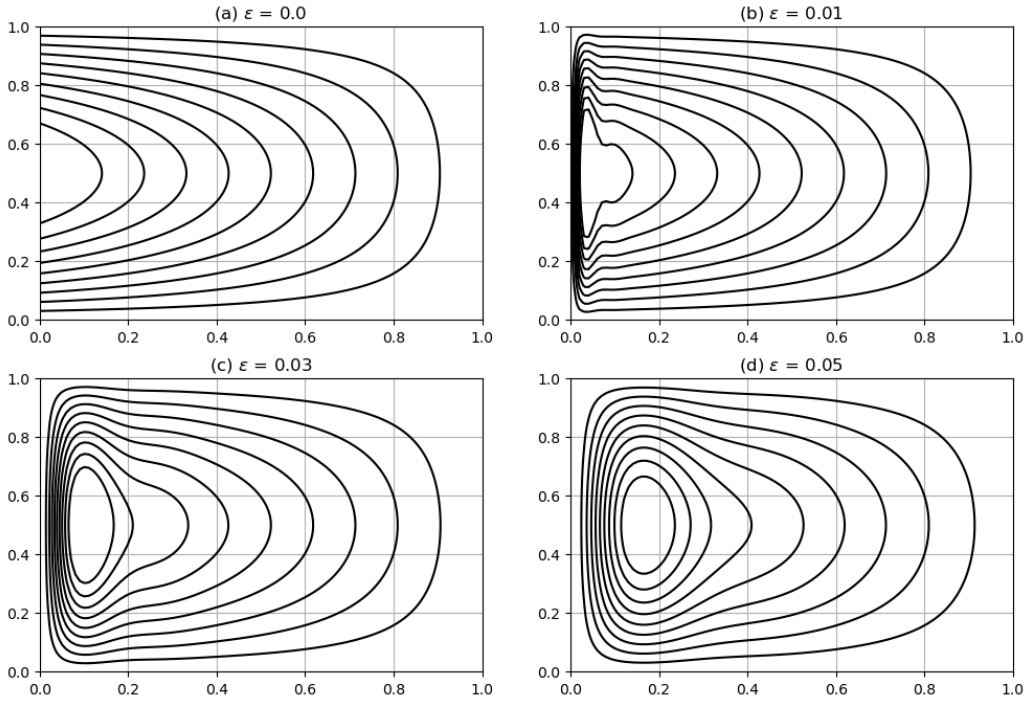

Figure 6.15: *Solutions of the Munk model for a single-gyre wind-induced flow for different values of ϵ. Note that for ϵ=0 the model reduces to the Sverdrup balance.*

where we have taken $C = 1$ as in Eq.(6.59) of the Stommel problem, the solution to the Munk problem is (a non-trivial algebraic exercise ...):

$$\hat{\psi} = \pi \, sin(\pi \hat{y}) \left\{ 1 - \hat{x} - e^{-\hat{x}/(2\epsilon)} \left[cos\left(\frac{\sqrt{3}\hat{x}}{2\epsilon} \right) + \frac{1-2\epsilon}{\sqrt{3}} sin\left(\frac{\sqrt{3}\hat{x}}{2\epsilon} \right) \right] + \epsilon e^{(\hat{x}-1)/\epsilon} \right\}. \tag{6.102}$$

The solution, for different values of ϵ, is shown in Fig. 6.15.

The Munk viscous boundary layer brings the tangential and the normal velocity to zero (Fig. 6.16).

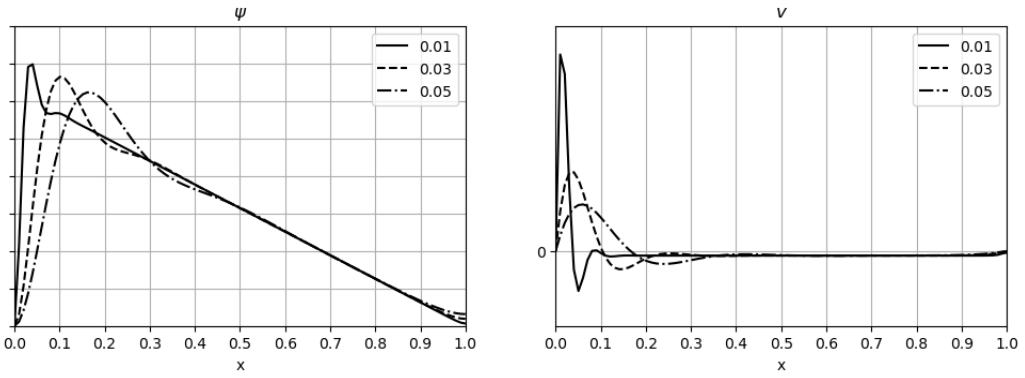

Figure 6.16: *Solutions of the Munk model for a single-gyre wind-induced flow for different values of ϵ. Plotted are the streamfunction ψ and the meridional velocity $v = \partial\psi/\partial x$ at the centre of the gyre. Note that the Munk model brings the velocity v to zero at the western boundary.*

The boundary layer width

What is the thickness of the Munk boundary layer? We have the following balance

$$\beta\frac{\partial\psi}{\partial x} \sim \nu\nabla^4\psi \tag{6.103}$$

$$\beta\frac{U}{L^2} \sim \nu\frac{U}{L^5} \tag{6.104}$$

$$\beta \sim \frac{\nu}{L^3}, \tag{6.105}$$

in the boundary layer lateral diffusion of momentum will be important and will extract momentum imparted by the wind stress. If lateral viscosity is important, the length scale will be $L = \mathcal{O}(\delta)$, and so the boundary layer width is given by

$$\boxed{\delta_M \sim \left(\frac{\nu}{\beta}\right)^{1/3}} \tag{6.106}$$

Figure 6.17: *Franklin wondered why journeys towards the east were faster than return trips on his voyages across the Atlantic Ocean between the Colonies and Europe. His curiosity led him to be the first to chart the Gulf Stream on 1786. Franklin was talking to his cousin, Timothy Folger, who was the captain of a merchant ship. He asked why it took ships like Folger's so much less time to reach America than it took official mail ships. It struck Folger that the British mail captains must not know about the Gulf Stream, with which he had become well-acquainted in his earlier years as a Nantucket whaler. Folger told Franklin that whalers knew about the "warm, strong current" and used it to help their ships track and kill whales. But the mail ships "were too wise to be counselled by simple American fishermen" and kept sailing against the current, losing time as they did so.*

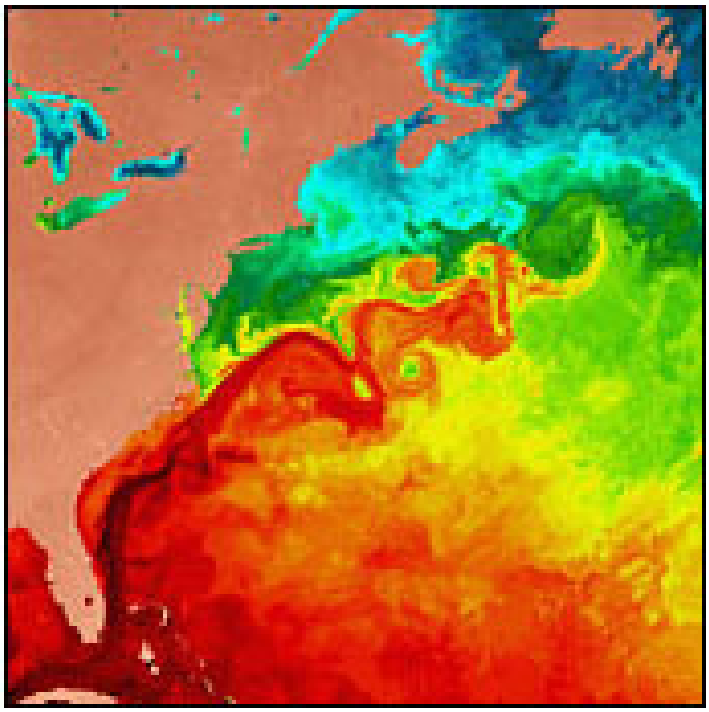

Figure 6.18: *A satellite image of the Gulf Stream.*

Neither the Stommel nor the Munk model are accurate representations of the real ocean. We need to include non-linearities and topographic effects to improve our solution.

The non-linear Stommel-Munk problem is

$$\frac{\partial \zeta}{\partial t} + J(\psi, \zeta) + \beta \frac{\partial \psi}{\partial x} = curl_z \boldsymbol{\tau}_T - r\nabla^2 \psi + \nu \nabla^2 \zeta. \tag{6.107}$$

And the steady non-linear Stommel-Munk problem is

$$J(\psi, \zeta) + \beta \frac{\partial \psi}{\partial x} = curl_z \boldsymbol{\tau}_T - r\nabla^2 \psi + \nu \nabla^2 \zeta. \tag{6.108}$$

The need for friction

Consider the steady barotropic flow

$$\frac{\mathrm{D}\,(f+\zeta)}{\mathrm{D}\,t} = F \tag{6.109}$$

satisfying

$$\boxed{\boldsymbol{u}\cdot\nabla q = curl_z\boldsymbol{\tau}_T + \text{Friction}}, \tag{6.110}$$

where $q = \nabla^2\psi + \beta y$ and the last term on the rhs represents frictional effects. $\boldsymbol{u}$ is divergent-free and we can integrate the lhs over some area A between two closed streamlines, ψ_1 and ψ_2. Using the divergence theorem[2] :

$$\int_A \nabla\cdot(\boldsymbol{u}q)\,\mathrm{d}A = \oint_{\psi_1} \boldsymbol{u}q\cdot\boldsymbol{n}\,\mathrm{d}l - \oint_{\psi_2} \boldsymbol{u}q\cdot\boldsymbol{n}\,\mathrm{d}l = 0. \tag{6.111}$$

Here $\boldsymbol{n}$ is the unit vector normal to the streamline so that $\boldsymbol{u}\cdot\boldsymbol{n} = 0$. The integral of the wind-stress curl over the area A will not be zero. This means that a balance between wind-stress curl and friction can only be achieved if every closed contour passes through a region where frictional effects are non-zero, and are important somewhere along the streamline path.

Thus, in the Stommel and Munk models, every streamline must pass through the frictional western boundary layer.

[2]Here we use the 2D divergence theorem for a vector field $F(x,y)$: $\iint_A \mathrm{div}\,F\,\mathrm{d}A = \oint_{\partial A} F\cdot\boldsymbol{n}\,\mathrm{d}l$

6.4 Westward intensification

PV balance interpretation

How does the potential vorticity balance work in Munk's model (which is combined with Sverdrup's model)?

Why do we find the boundary current on the western side rather than the eastern side, or even within the middle of the basin (if considering Stommel's bottom friction)?

In the Sverdrup interior of a subtropical gyre, when the wind causes Ekman pumping, the water columns are squashed, they move equatorward to lower planetary vorticity.

To return to a higher latitude, there must be forcing that puts the higher vorticity back into the fluid. This cannot be in the form of planetary vorticity, since this is already contained in the Sverdrup balance. Therefore, the input of vorticity must affect the relative vorticity.

Consider a western boundary current for a Northern Hemisphere subtropical gyre, with friction between the current and the side wall (Munk's model). The effect of the side wall is to reduce the boundary current velocity to zero at the wall. Therefore, the boundary current has positive relative vorticity. This vorticity is injected into the fluid by the friction at the wall, and allows the current to move northward to higher Coriolis parameter f.

On the other hand, if the narrow jet returning flow to the north were on the eastern boundary, the side wall friction would inject negative relative vorticity, which would make it even more difficult for the boundary current fluid to join the interior flow smoothly.

Therefore, vorticity arguments require that frictional boundary currents be on the western boundary. You can go through this exercise for subpolar gyres as well as for both types of gyres in the Southern Hemisphere and will find that a western boundary current is required in all cases!

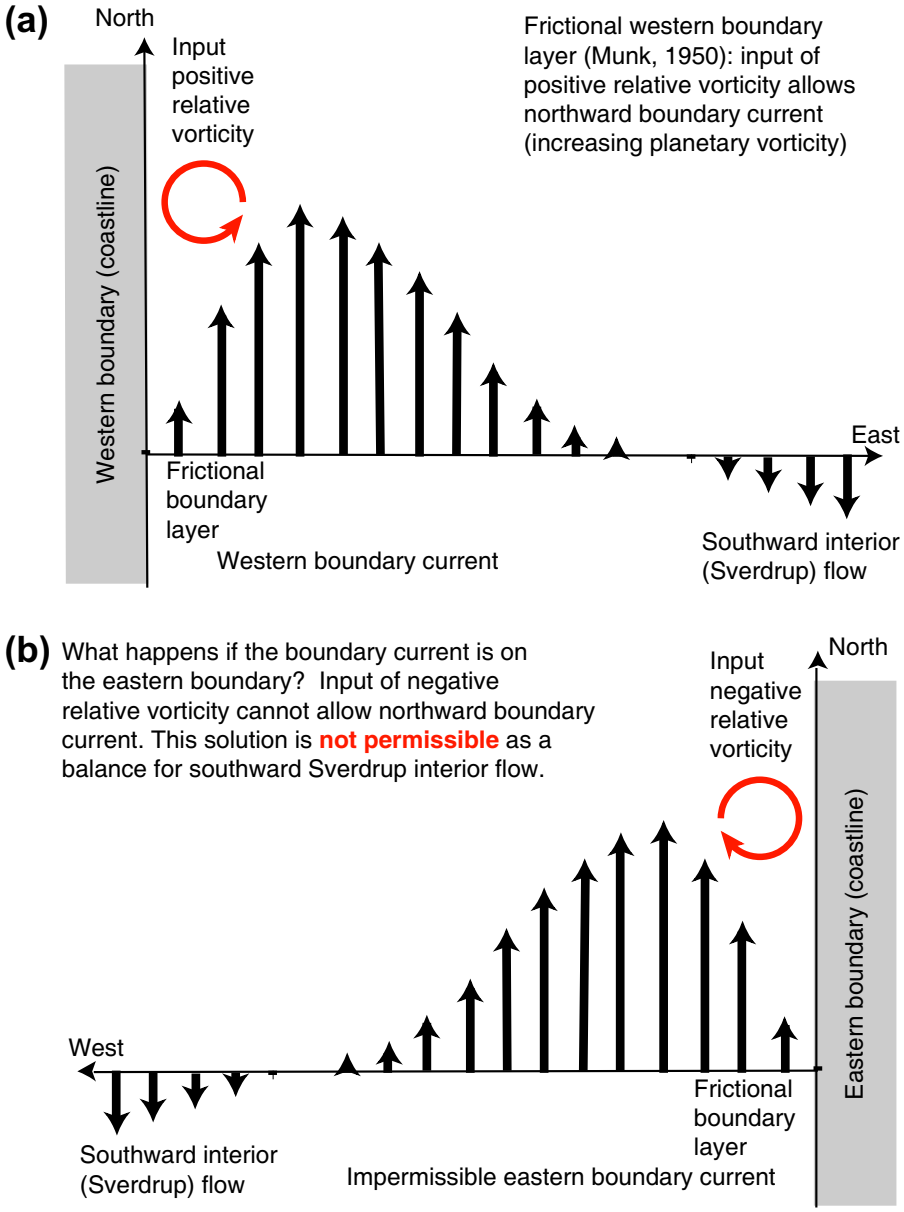

Figure 6.19: *(a) Vorticity balance at a western boundary, with side wall friction (Munk's model). (b) Hypothetical eastern boundary vorticity balance, showing that only western boundaries can input the positive relative vorticity required for the flow to move northward. [from Talley et al. (2011)]*

Western intensification understood as westward drift

Here we'll give a slightly different explanation of why the boundary current is in the west. It is not really a different explanation, because the cause is still **differential rotation**, but we'll think about it quite differently. We'll see the effect of differential rotation is to make patterns propagate to the west, and hence the response to the wind's forcing piles up in the west and produces a boundary current there.

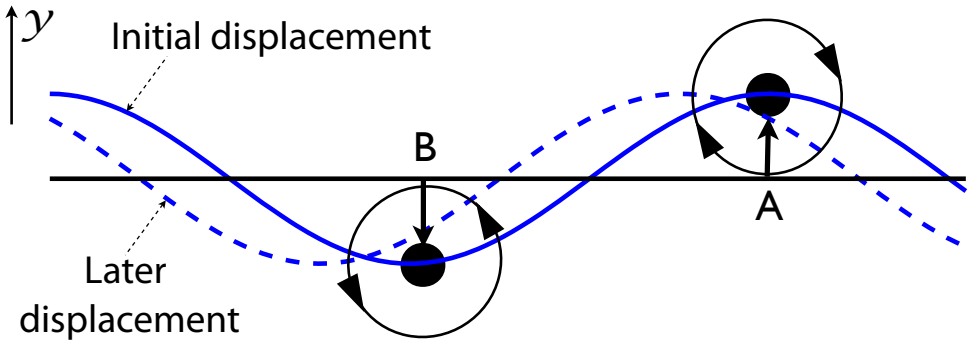

Figure 6.20: *If parcel A is displaced northwards then its clockwise spin increases, causing the northwards displacement of parcels that are to the west of A. A similar phenomena occurs if parcel B is displaced south. Thus, the initial pattern of displacement propagates westward. [from Vallis (2006)]*

Let's now imagine a line of parcels (Fig. 6.20). Suppose we displace parcel 'A' northwards. Because the Earth's spin is anti-clockwise (looking down on the North Pole) and this increases as the parcel moves northward, then the parcel must spin more in a clockwise direction in order to preserve its total vorticity

$$q = f + \zeta. \tag{6.112}$$

This spin will have the effect of moving the fluid that is just to west of the original parcel northwards, and then this will spin more clockwise, moving the fluid to its left northwards, and so on. The northwards displacement thus propagates *westward*, whereas parcels to the east of the original displacement are returned to their original position so that there is no systematic propagation to the east. Similarly, a parcel that is displaced southwards (parcel B) also causes the pattern to move westwards. We have just described the westward propagation of a simple *Rossby wave*, but the same effect occurs with more complex patterns and in particular, with the gyre as a whole.

Thus, imagine that an east-west symmetric gyre is set up, with the winds and friction in equilibrium, as in an f-plane. Differential rotation then tries to move the pattern westward, but of course the entire pattern cannot move to the west because there is a coastline in the way! The gyre thus squashes up against the western boundary creating an intense western boundary current.

This way of viewing the matter serves to emphasize that **it is not frictional effects that cause western intensification; rather, frictional effects allow the flow to come into equilibrium with an intense western boundary current, with the ultimate cause being the westward propagation due to differential rotation.**

In fact, the location of the boundary layer, on the west, does not depend on the sign of the wind-stress curl (the sign is reversed in a subpolar gyre and the flow is southward within a western boundary current) nor on the sign of the Coriolis parameter (think about what happens in the southern hemisphere where $f < 0$). The western location depends on β, which is always positive (Fig. **??**). What would happen if we change the direction of rotation of the Earth? β would be negative, Rossby waves would travel eastward and the boundary layer would be located on the eastern side of the basin.

The Stommel & Munk models of the Wind-Driven Circulation

– The Model

1. The model uses the vertically integrated planetary-geostrophic equations (or a homogeneous fluid) with nonlinearities neglected.
2. The model uses a flat bottomed ocean.
3. - In the Stommel model, bottom friction is parameterized by a *linear drag*.
   - In the Munk model, lateral friction is parameterized by a *Newtonian harmonic viscosity* .

– Solution

1. The transport in the Sverdrup interior is equatorwards for an anti-cyclonic wind-stress-curl.
2. The Sverdrup transport is exactly balanced by a poleward transport in a westward boundary layer.
3. The boundary layer satisfies mass conservation, and must be a *western* boundary layer for friction to provide a force of opposite sign as the motion in the interior.

   The boundary layer is a *frictional boundary layer*.
4. The western location does not depend on the sign of the Coriolis parameter nor on the sign of the wind stress. The location does depend on the sign of β, and so on the direction of rotation of the Earth.
5. - In the Stommel model the balance in the western boundary layer is between $r\nabla^2\psi$ and $\beta\frac{\partial\psi}{\partial x}$. The boundary layer width is $\delta_S = \left(\frac{r}{\beta}\right)$. If r, the inverse frictional time, is $1/20$ days^{-1}, then $\delta_S \approx$60 km.
   - In the Munk model the balance in the western boundary layer is between $\nu\nabla^4\psi$ and $\beta\frac{\partial\psi}{\partial x}$. The boundary layer width is $\delta_M = \left(\frac{\nu}{\beta}\right)^{1/3}$.

6.5 Topographic effects on western boundary currents

We have so far assumed a flat ocean bottom in order to derive the equations of the Sverdrup, Stommel and Munk models. This allowed us to eliminate the depth-integrated pressure gradient force when taking the curl of the depth-integrated momentum budget. But the ocean is certianly not flat, and sloping sidewalls will actually change the behaviour of western boundary currents. They can even become inviscid if the flow is preserving its potential vorticity by flowing along f/h contours. If the ocean is flat, then a meridional flow within a boundary layer exists thanks to frictional effects permitting the flow to cross f contours. If sidewalls are sloping then the flow can move quasi-northward (along f/h contours) preserving its potential vorticity.

6.5.1 Bottom pressure stress

We now consider the effects of topography and stratification on the circulation of a wind-driven gyre. Interactions of pressure with a variable topography can generate a meridional flow. The vorticity balance of a depth-integrated flow now possesses and extra term describing the influence of topography on the flow.

Let's define $h = h(x, y)$ and let's consider a stratified ocean in which density is not a constant. The momentum equation in planetary-geostrophic approximation is

$$\boldsymbol{f} \times \boldsymbol{u} = -\nabla\phi + \boldsymbol{F} \tag{6.113}$$

where $\boldsymbol{F}$ represents both frictional and wind forcing terms. Integrating this over the entire depth of the water column

$$\boldsymbol{f} \times \overline{\boldsymbol{u}} = -\int_{\eta_B}^{0} \nabla\phi \, \mathrm{d}z + \overline{\boldsymbol{F}} \tag{6.114}$$

where $\overline{x} = \int_{\eta_B}^{0} x \, \mathrm{d}z$. Now remember the Leibnitz rule:

$$\nabla \int_{\eta_B}^{0} \phi \, \mathrm{d}z = \int_{\eta_B}^{0} \nabla\phi \, \mathrm{d}z + \phi_0 \nabla\eta_T - \phi_B \nabla\eta_B, \tag{6.115}$$

where the second term on the rhs vanishes given that $\eta_T = z = 0$ at the top. For our purpose:

$$\int_{\eta_B}^{0} \nabla\phi \, \mathrm{d}z = \nabla \int_{\eta_B}^{0} \phi \, \mathrm{d}z + \phi_B \nabla\eta_B, \tag{6.116}$$

and so we write the vertically integrated momentum equations as

$$\boldsymbol{f} \times \overline{\boldsymbol{u}} = -\nabla \int_{\eta_B}^{0} \phi \, \mathrm{d}z - \phi_B \nabla\eta_B + \overline{\boldsymbol{F}}. \tag{6.117}$$

The second term on the rhs is the stress in the fluid due to the correlation between pressure gradient and topography. It is called bottom *form drag*.

If we rewrite the vertical integral of the pressure:

$$\int_{-h}^{0} \phi \, \mathrm{d}z = (\phi z)|_{-h}^{0} - \int_{-h}^{0} z(\partial\phi/\partial z)\mathrm{d}z = \phi_B h + \int_{-h}^{0} z\rho g \, \mathrm{d}z = \phi_B h + E, \tag{6.118}$$

where we have used hydrostasy $\partial\phi/\partial z = -\rho g$ and defined the vertically-integrated potential energy $E = g \int_{-h}^{0} z\rho \, \mathrm{d}z$.

Our vertically integrated momentum thus become

$$\begin{aligned}
\boldsymbol{f} \times \overline{\boldsymbol{u}} &= -\nabla \int_{\eta_B}^{0} \phi \, \mathrm{d}z - \phi_B \nabla\eta_B + \overline{\boldsymbol{F}} && (6.119)\\
&= -\nabla \int_{\eta_B}^{0} \phi \, \mathrm{d}z + \phi_B \nabla h + \overline{\boldsymbol{F}} && (6.120)\\
&= -\nabla\Big(\phi_B h + E\Big) + \phi_B \nabla h + \overline{\boldsymbol{F}} && (6.121)\\
&= -h\nabla\phi_B - \nabla E + \overline{\boldsymbol{F}}. && (6.122)
\end{aligned}$$

Where we have used $\nabla\eta_B = -\nabla h$, taking the top of the ocean at $z = 0$ and h the fluid column. To obtain a vorticity balance equation, and eliminating the pressure terms, we divide by h and take the curl. After using the streamfunction$(u, v) = (-\partial\psi/\partial y, \partial\psi/\partial x)$:

$$\boxed{J\Big(\psi, f/h\Big) + J\Big(h^{-1}, E\Big) = curl_z(\overline{\boldsymbol{F}}/h)} \tag{6.123}$$

Assuming a flat bottom and constant density, we see that a torque provided by the wind stress balances the torque introduced by bottom friction and a torque related to the change in planetary vorticity, just as in Stommel. However, now an extra term appears which is related to the combined effect of stratification and topographic variations (or Joint Effect of Baroclinicity And Relief - JEBAR - term): $J\left(h^{-1}, E\right)$. For a constant h, the JEBAR term vanishes and we recover the Stommel problem

$$\beta \frac{\partial \psi}{\partial x} = curl_z \overline{\boldsymbol{F}} \tag{6.124}$$

An alternative derivation accounting for the effect of topography and stratification is given by eliminating the potential energy term instead of the bottom pressure term. Going back to

$$\boldsymbol{f} \times \overline{\boldsymbol{u}} = -\nabla \int_{\eta_B}^{0} \phi \, \mathrm{d}z - \phi_B \nabla \eta_B + \overline{\boldsymbol{F}} \tag{6.125}$$

and taking the curl gives[3]

$$\beta \overline{v} = curl_z \overline{F} - curl_z(\phi_B \nabla \eta_B) = curl_z \overline{F} - J\left(\phi_B, \eta_B\right). \tag{6.126}$$

The last term on the rhs is the bottom pressure-stress curl, or form-drag curl, or bottom pressure torque. And now this equation holds for both a homogeneous and stratified fluid.

For a homogeneous, frictionless and unforced gyre, this reduces to

$$\boxed{\beta \overline{v} = -J\left(\phi_B, \eta_B\right)} \tag{6.127}$$

or

$$\beta \overline{v} = -\nabla \phi_B \times \nabla \eta_B \tag{6.128}$$

There can be a meridional flow only if pressure gradient has a component parallel to topographic contour (the isobars are not aligned with topographic contours), and the term on the rhs is non-zero. The meridional flow is driven by the curl of the form drag. In a flat-bottomed ocean, the form drag is zero, and the meridional flow must be forced or viscous.

[3] $curl_z(h \nabla \phi_B) = curl_z(\phi_B \nabla \eta_B)$

f/h contours

If we consider an ocean where both forcing and friction are absent, and assuming an homogeneous gyre, the vorticity balance simplifies to

$$\boxed{J\left(\psi, f/h\right) = 0} \tag{6.129}$$

In an inviscid, unforced, and unstratified flow, ψ is a function of f/h, and streamlines of constant ψ and (f/h) contours coincide. In this case, the depth-integrated large-scale flow must follow f/h contours. The f/h contours form the characteristics of the differential equation above. This is called a *free mode*, driven solely by the bottom pressure-stress curl.

This is a statement about the balance between the vortex stretching by changes in topography and change in planetary vorticity of the fluid column. Consider a sloping sidewall, if a water column moves down the slope it will stretch in the vertical and increase its vorticity $(f + \zeta)$. On a

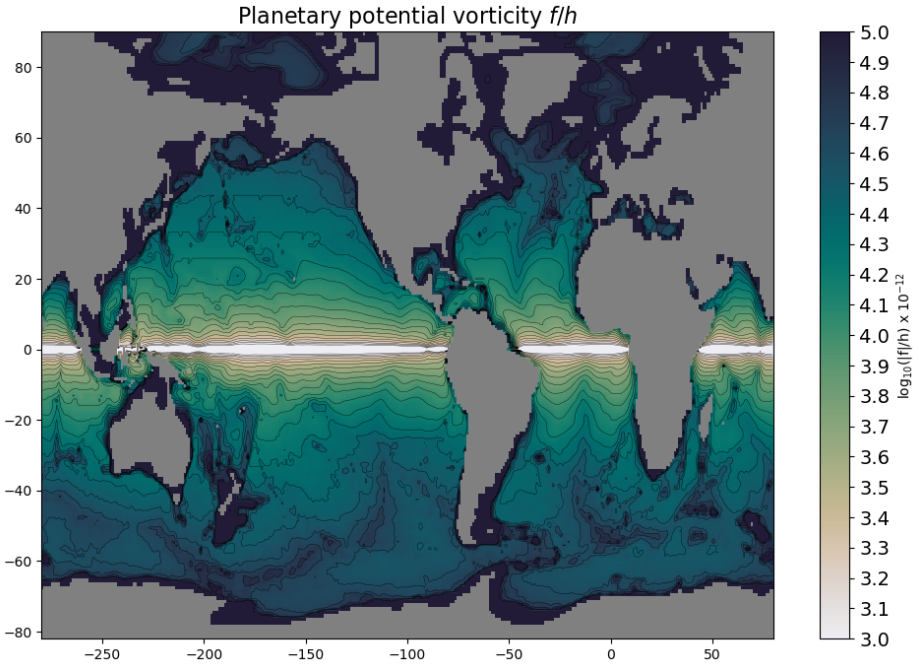

Figure 6.21: *Contours of planetary potential vorticity, f/h. Shown is $log_{10}(|f|/h\,[10^{-12}\,m^{-1}s^{-1}])$. For constant h, the f/h contours would follow latitude circles. The influence of topography on the depth-averaged flow is small in the tropics but becomes large at higher latitudes. In the Atlantic Ocean, the imprint of the mid-Atlantic ridge can be seen in the region of the subtropical gyres.*

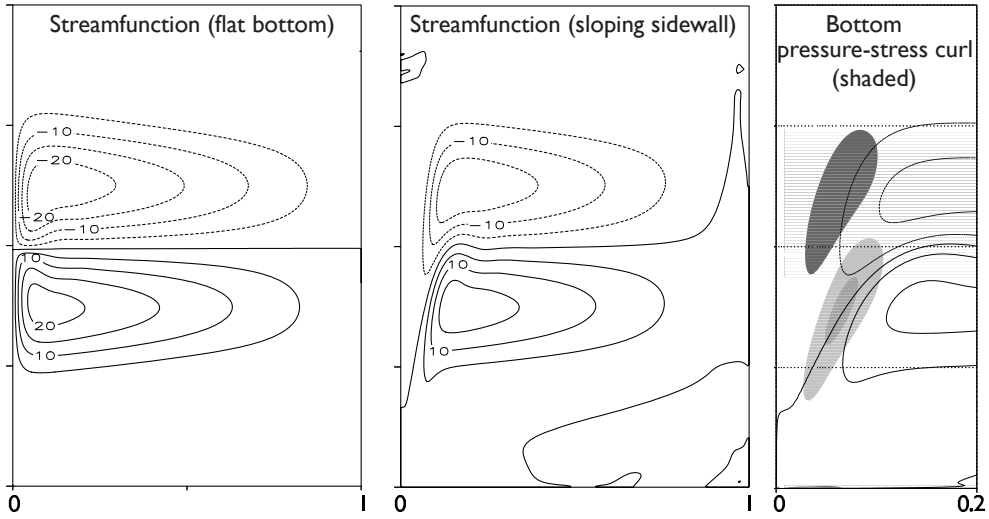

Figure 6.22: *Numerical results for a homogeneous problem, flat bottom domain and a domain with sloping western sidewall. The shaded regions in the right panels show the regions where bottom pressure-stress curl is important in the meridional flow of the western boundary current. [from Vallis (2006)]*

basin scale this will be balanced by changes in f rather than changes in ζ, so the PV balance reduces to $q = f/h$. In order to conserve PV, the column will be displaced meridionally, moving along f/h contours. The new f will be modulated by the thickness change h_2/h_1. For a constant h, f/h contours would follow latitude circles.

This vorticity conservation principle is shown by the linear vorticity equation:

$$\beta v = f\frac{\partial w}{\partial z} + \frac{\partial}{\partial z}\left(\tau_x^y - \tau_y^x\right) \tag{6.130}$$

Now, integrating vertically the vertical velocity does not vanish (assuming that $w_T = 0$):

$$\underbrace{\beta\overline{v}}_{\substack{\text{change in}\\ \text{planetary vorticity}}} = \underbrace{curl_z\boldsymbol{\tau}_T}_{\substack{\text{torque by}\\ \text{the wind}}} - \underbrace{curl_z\boldsymbol{\tau}_B}_{\substack{\text{torque by}\\ \text{bottom friction}}} - \underbrace{fw_B}_{\substack{\text{stretching of}\\ \text{water column}}} \tag{6.131}$$

Now that this is clear, we can go back to the vertically integrated vorticity balance

$$\beta\overline{v} = curl_z\overline{F} - curl_z(\phi_B\nabla\eta_B), \tag{6.132}$$

and considering both surface forcing and bottom drag we have the follow-

ing vorticity budget for the vertically integrated flow

$$\underbrace{\beta\overline{v}}_{1} = \underbrace{curl_z\overline{\boldsymbol{\tau}}_T}_{2} - \underbrace{curl_z\overline{\boldsymbol{\tau}}_B}_{3} - \underbrace{curl_z(\phi_B\nabla\eta_B)}_{4}. \tag{6.133}$$

(1)+(2) is the Sverdrup balance; (1)+(2)+(3) is the Stommel problem. (4) introduces the bottom pressure torque.

The torque by the wind stress drives a meridional flow across f-lines (Fig. 6.23), as in Sverdrup balance. The western boundary layer is then dominated by a balance between the meridional flow (βv) and the bottom pressure-stress curl. Only where the flow crosses f/h contours is friction needed (Fig. 6.23b). This happens where f/h contours converge and friction helps the flow move across f/h contours. In a flat-bottomed case, friction would be necessary all along the boundary layer in order to cross f contours(Fig. 6.23a).

The fact that the bottom pressure torque can play a more dominant role than frictional torque for the vorticity balance in the western boundary current questions the physical relevance of Stommel's model.

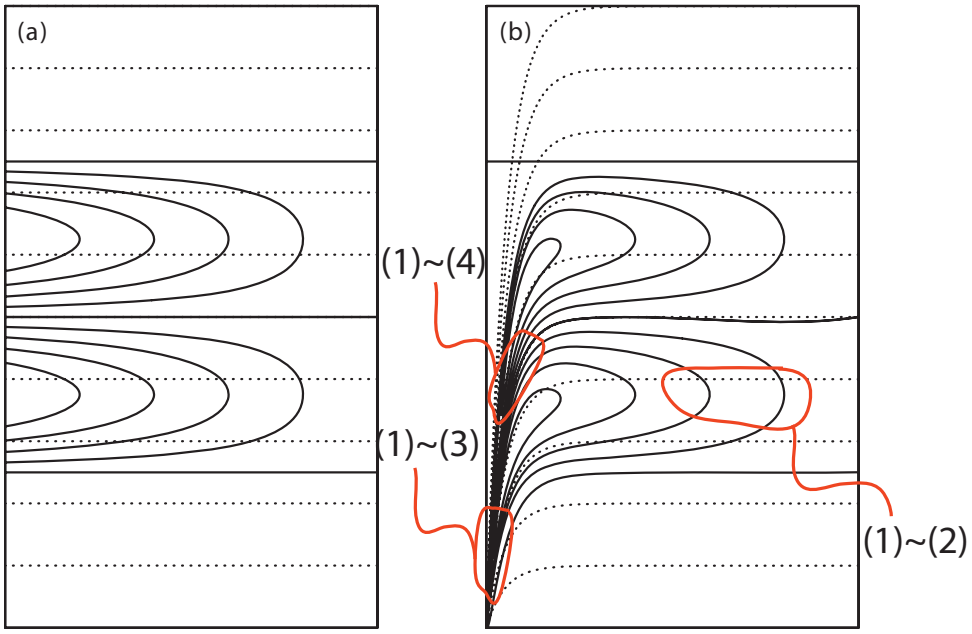

Figure 6.23: *The two-gyre Sverdrup flow for a flat-bottomed domain and a domain with sloping sidewalls. f/h contours are dotted. [adapted from Vallis (2006)].*

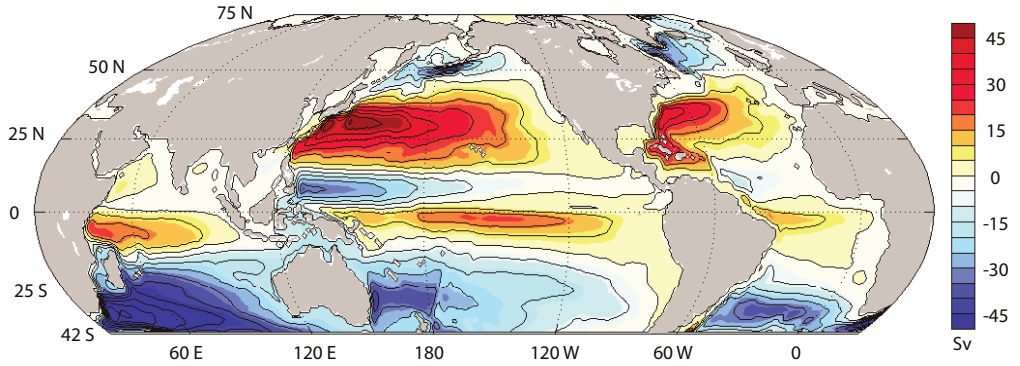

Figure 6.24: *A realistic barotropic streamfunction. [adapted from Vallis (2006)].*

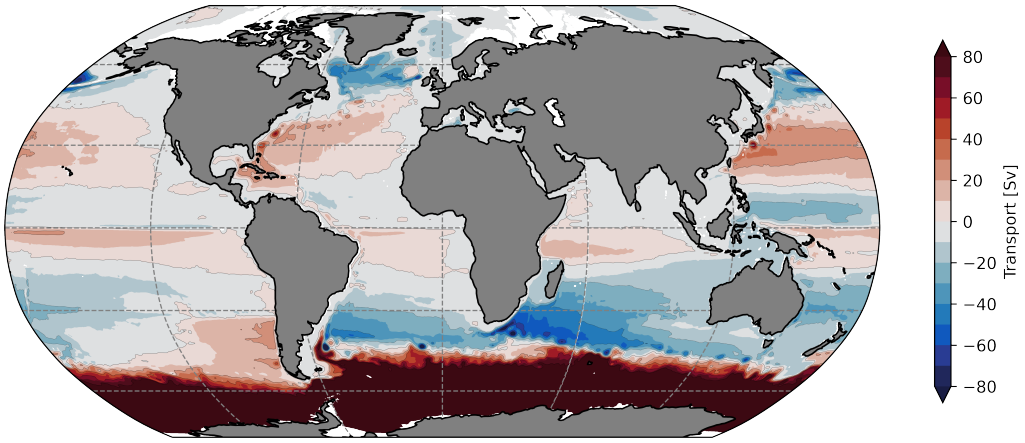

Figure 6.25: *The quasi-barotropic streamfunction from MOM at 0.25 degree resolution (time-mean for the period 2013-2017).*

Exercices

1. Compute the Sverdrup circulation in a rectangular ocean ($0 < x < L_x, 0 < y < L_y$) forced by a zonal wind stress

$$\tau_0^x(y) = -\tau_0 \, cos\frac{\pi y}{L_y}, \quad \tau_0^y = 0.$$

Take $\tau_0 > 0$ and a constant β. Show that the Sverdrup transport velocities and the streamfunction are

$$\begin{aligned} U &= -(L_x - x)\,\frac{\tau_0 \pi^2}{\beta {L_y}^2}\, cos\frac{\pi y}{L_y}, \\ V &= -\frac{\tau_0 \pi}{\beta L_y}\, sin\frac{\pi y}{L}, \\ \psi(x,y) &= (L_x - x)\frac{\tau_0 \pi}{\beta L_y}\, sin\frac{\pi y}{L_y}. \end{aligned}$$

Take the following parameters: L_x=5000 km, L_y=4000 km, τ_0=10^{-4}m^2 s^{-2} (the reference density ρ_0 is absorbed into the turbulent stress vector), $f = f_0 + \beta y$, with $f_0 = 7 \times 10^{-5}\ s^{-1}$, $\beta = 2 \times 10^{-11}\ m^{-1}s^{-1}$.

Show that the maximum transport across the basin width is $(\pi B/L)\tau_0/\beta$ and amounts to ∼20 Sv.

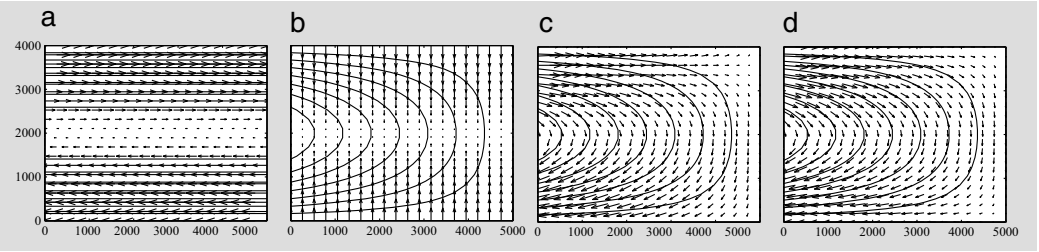

Figure 6.26: *(a) Wind stress pattern. (b) The transports due to the Ekman layer. (c) The geostrophic part with $U_g = U - U_E, V_g = V - V_E$ (note that $U_E = 0$). (d) The Sverdrup transport. The Sverdrup transport streamfunction ψ is shown in all plots.*

2. What happens, and why, to the transport at $\text{curl}_z\boldsymbol{\tau} = 0$?

3. Compute the Ekman, geostrophic and Sverdrup transports for the following parameters. What is the total flux through the basin?

- θ = 35°N
- $\tau^x = 10^{-1}\ Nm^{-2}$
- $\tau^y = 0$
- L_y =1000 km; L_x=5000 km
- f=$10^{-4}\ s^{-1}$
- $\beta = 2 \times 10^{-11}\ m^{-1}s^{-1}$

4. Compute the Sverdrup subtropical meridional transport in the North Atlantic for the given parameters. What is the typical size of the interior velocity (cm s^{-1}) if the transport is carried over the upper 1 km of the ocean and the basin is 3000 km wide?

   - θ = 35°N
   - $\tau^x = 0.1\ Nm^{-2}$
   - $\tau^y = -0.1\ Nm^{-2}$
   - $curl_z \boldsymbol{\tau} = -0.1 \times 10^{-6}\ N\ m^{-3}$
   - $\rho_0 = 10^3\ kgm^{-3}$
   - $\beta = 2 \times 10^{-11}\ m^{-1}s^{-1}$

Bibliography

Farneti, R., A. Stiz, and J. Ssebandeke, Improvements and persistent biases in the southeast tropical Atlantic in CMIP models, *npj Climate and Atmospheric Science*, *x*, xx–xx, 2022.

Gill, A. E., *Atmosphere-Ocean Dynamics*, *International Geophysics Series*, vol. **30**, 662 pp., Academic Press, 1982.

Levitus, S., Ekman volume fluxes for the World Ocean and individual ocean basins, *J. Phys. Oceanogr.*, *18*, 271–279, 1988.

Olbers, D., J. Willebrand, and C. Eden, *Ocean Dynamics*, Springer-Verlag, 704 pp, 2012.

Talley, L., G. L. Pickard, W. J. Emery, and J. H. Swift, *Descriptive Physical Oceanography*, Academic Press, 560 pp, 2011.

Vallis, G. K., *Atmospheric and Oceanic Fluid Dynamics*, Cambridge Univ. Press, 745 pp, 2006.